Electronic Supplementary Material (ESI) for Inorganic Chemistry Frontiers.

Electronic Supplementary Information

Employing a template synthesis to access diastereopure Np(IV) and U(IV) complexes and analysis of their 5*f* orbitals in bonding

Stephanie H. Carpenter,[a‡] María J. Beltrán-Leiva,[b‡] Shikha Sharma,[a] Micahel L. Tarlton,[a] James T. Moore,[a] Andrew J. Gaunt,[a] Enrique R. Batista,[b*] Aaron M. Tondreau,[a*] and Ping Yang[b*]

[a]Chemistry Division, Los Alamos National Laboratory, Los Alamos, New Mexico 87545, United States
[b]Theorectical Division, Los Alamos National Laboratory, Los Alamos, New Mexico 87545, United States

Corresponding Authors
Aaron M. Tondreau – *Los Alamos National Laboratory, Los Alamos, New Mexico 87545, United States;* orcid.org/0000-0003-0440-5497; Email: tondreau_a@lanl.gov
Ping Yang – *Los Alamos National Laboratory, Los Alamos, New Mexico 87545, United States;* orcid.org/0000-0003-4726-2860; Email: pyang@lanl.gov
Enrique R. Batista – *Los Alamos National Laboratory, Los Alamos, New Mexico 87545, United States;* orcid.org/0000-0002-3074-4022; Email: erb@lanl.gov

Table of Contents (S2)

1. Experimental Considerations

Caution! *Depleted uranium (primary isotope ^{238}U, $t_{1/2} = 4.47 \times 10^9$ years) is a weak α-emitter. Neptunium (^{237}Np, $t_{1/2} = 2.144 \times 10^6$ years) is an α-emitter and its ^{233}Pa daughter is a β- and γ-emitter, where both isotopes present serious health threats. Only persons trained to handle such material should perform work and only in an adequately prepared laboratory setting. All manipulations of neptunium chemistry were conducted in a radiation laboratory equipped with high efficiency particulate air (HEPA) filtered hoods and in a negative pressure glovebox with a purified helium atmosphere. Additional safeguards used to monitor radiation levels include, but are not limited to, continuous air monitoring, hand-held radiation monitoring devices, and hand, foot, and full body contamination monitoring. Due to radiological hazards ^{237}Np presents, it is not possible to have elemental analyses performed by a third-party laboratory.*

1.1 Materials. The solvent THF was dried over molecular sieves and sodium-potassium alloy (NaK) prior to use; the solvents pentane, fluorobenzene, C_6H_6 and C_6D_6 were dried over molecular sieves prior to use. C_6D_6 was purchased from Cambridge Isotope Laboratories. UCl_4,[1] $(dme)_2NpCl_4$,[2] 4,7-dimethyl-1,3-bis(1-methylethyl)-1*H*-indene (1,3-iPr_2-4,7-Me_2-C_9H_3),[3] and trimethylsilyl-(di-*tert*-butyl)-phosphine ($^tBu_2PSiMe_3$)[4, 5] were synthesized from previously reported procedures. 2,6-pyridinedicarboxaldehyde (97%), 4,4'-di-*tert*-butyl-2,2'-bipyridyl (dtbpy), and potassium bis(trimethylsilyl)amide (KHMDS) were purchased from commercial sources (*e.g.*, Sigma) and used as received after degassing and bringing into the inert atmosphere gloveboxes.

1.2 General Considerations. All air- and moisture-sensitive ^{238}U manipulations were carried out in an MBraun dry box containing a purified argon atmosphere. All air- and moisture-sensitive ^{237}Np manipulations were carried out in an MBraun negative-pressure dry box containing a purified helium atmosphere. ^1H and ^{31}P NMR spectra were recorded on a Bruker Avance 400 MHz spectrometer operating at 400.132 MHz and 161.978 MHz, respectively. All ^1H chemical shifts are reported relative to $SiMe_4$. Paramagnetically broadened resonances have the peak-width at half-height recorded in parenthesis following the δ; integration and splitting is reported when able to assign the resonances with reasonable confidence, such as in the case of the PtBu2 moiety. CHN analyses were conducted by the University of Rochester CENTC Elemental Analysis Facility, B14 Hutchison Hall, 120 Trustee Road, Rochester, NY 14627 and analyzed by William W. Brennessel. Uranium UV/Vis/NIR spectra were collected at RT on a Cary 5000 UV-Vis-NIR spectrophotometer from Agilent Technologies. Neptunium UV/Vis/NIR spectra were collected at RT on a Varian Cary 6000i UV/vis/NIR spectrometer. Extreme caution must be used when making solution neptunium UV/Vis/NIR samples to ensure no radiological contamination occurs on the outside of the cuvette, and previously described methods for the handling of such samples were used.[6]

Single crystals of uranium complexes suitable for X-ray diffraction were coated with Krytox™ in a dry box, placed on a nylon loop and then transferred to a goniometer head of a Bruker D8 Quest diffractometer equipped with a Mo Kα X-ray tube (λ = 0.01073 Å) IμS 3.0 Microfocus source X-ray generator.[7] Single crystals of neptunium complexes suitable for X-ray diffractions were coated with Krytox™ and mounted inside a 0.5 mm quartz capillary from Charles Supper. To prevent radiation contamination, the quartz capillaries were inserted into a test tube via silicon stoppers to allow for handling of the capillaries while inserting crystalline material. As the capillaries are too long to mount on a goniometer head, the capillaries are carefully cut with nail clippers to a more appropriate size prior to sealing with hot capillary wax. After removal from the dry box, the capillaries are coated in clear nail polish to provide shatter-resilience. The capillaries are then transferred to a goniometer head of a Bruker D8 Quest diffractometer equipped with a Mo Kα X-ray tube (λ = 0.01073 Å) IμS 3.0 Microfocus source X-ray generator.[7] A hemisphere routine was used for data collection and determination of lattice constants. The space group was identified and the data were processed using the Bruker SAINT+ program and corrected for absorption using SADABS.[8-10] The structures were solved using direct methods (SHELXS) completed by subsequent Fourier synthesis and refined by full-matrix least-squares procedures.[11, 12] Olex2 software was used as the graphical interface.[13, 14] Crystallographic data for all structures is available from the Cambridge Structural Database.

1.3 Computational Descriptions. *Density Functional Theory (DFT) Calculations*. Geometry optimizations of complexes **1-4** were performed on AMS version 2022.101 with no symmetry or geometry constraints.[15] Additionally, models for **1** and **2** were also optimized by removing the methyl groups from the ONO ligand. At first, the level of theory consisted of the generalized gradient approximation (GGA) Perdew-Burke-Ernzerhof (PBE) functional in conjuction with Slate-type basis functions (STO) triple-ζ plus polarization (TZP).[16] The resulting optimized coordinates were used as input for a second optimization step using the hybrid Becke, 3-parameter, Lee-Yang-Parr exchange-correlation B3LYP functional (25% of Hartree-Fock (HF) exchange).[17, 18] Scalar relativistic effects (SR) were incorporated through the zeroth-order relativistic approximation (ZORA) Hamiltonian.[19] The optimized structures were confirmed to be true minima by analytical vibrational frequency calculations. The natural localized molecular orbital (NLMO) analysis was further performed in the standalone version of NBO 7.0 to get a more accurate picture of the bonding in these systems.[20] The extended transition state (ETS) combined with the natural orbitals for chemical valence (NOCV) theory, along with the second-order perturbation analysis in NBO basis were also performed to analyze the nature of the different An-ligand interactions and to estimate their energetic importance.[21] Time-dependent DFT (TD-DFT) calculations were carried out to identify the transitions involved in the absorption spectra. The lowest 300 excitations were obtained employing the PBE, as well as the B3LYP, functionals.

Wavefunction Calculations. All the complexes were subjected to wavefunction calculations using the ORCA 5.0.3 package.[22] In a first step, DFT densities obtained at B3LYP/def2-TZVP level of theory were calculated to serve as starting points for the multiconfigurational calculations.[23] The metal center was described with the SARC-DKH-TZVP basis set.[24] SR effects were incorporated via the second-order Douglas-Kroll-Hess (DKH) Hamiltonian.[25] In a second step, state average (SA) complete active space self-consistent field (CASSCF) calculations were performed using the basis sets and SR approximation previously defined.[26] At this point, the static correlation that arises from the unpaired electrons being distributed among near-degenerate 5*f* shell is accounted for. The first active space consisted of n electrons (n = 2,3 for U^{4+} and Np^{4+}, in seven 5*f* orbitals (CAS(n,7)) (**Figure S1**). All the possible configuration state functions (CSF) were considered. For the uranium complexes **1** and **3**, 21 and 28 CSF were included for the triplets and singlets, respectively. In the case of the neptunium complexes **2** and **4**, 35 and 112 CSF were included for the quartet and doublets, respectively. A second active space that incorporates ligand orbitals was also pursued. The idea was to incorporate their bonding and antibonding counterparts in order to keep the balance of the active space. These orbitals corresponded to 2 low-lying bonding orbitals plus their antibonding equivalents coming from the dtbpy and indenide ligands (CAS(n+4,11) (**Figure S2**). Convergence was achieved for the systems containing the indenide ligand. However, for those having coordinated the dtbpy ligand, just the minimum active space converged. This means that more ligand orbitals need to be included into the active space, which becomes impractical from a computational perspective. After the CASSCF calculations converged, the N-electron valence state second-order perturbation theory (NEVPT2) method was employed to account for the so-called dynamic correlation.[27] Finally, the spin-orbit (SO) coupling was included via quasi-degenerate perturbation theory (QDPT) employing the NEVPT2 diagonal energies.

Spectra Broadening. The SO-CASSCF/NEVPT2 calculated energies and oscillator strengths were subjected to Gaussian broadening. Initially, the energies in wavenumbers were considered to perform the broadening process with a full width at half-maximum (FWHM) equal to 227 cm^{-1} (~0.03 eV). As final step, the energies were converted to wavelengths (nm) to match the experimental data.

1.4 Synthesis of ($^{(tBu2P)}$ONO)$NpCl_2$(dtbpy), 2. A 20 mL scintillation vial was loaded with a stir bar, $(dme)_2NpCl_4$ (20.9 mg, 0.037 mmol), 2,6-pyridinedicarboxaldehyde (5.1 mg, 0.038 mmol) and THF (1 mL). The reaction was allowed to mix at room temperature for 5 minutes, wherein the solution turns pale pink (**Figure S18**). The additions of $^tBu_2PSiMe_3$ (18.2 mg, 0.083 mmol) to this pale pink solution resulted in a color change to golden yellow (**Figure S19**), where this solution was allowed to mix at room temperature for 5 minutes. All volatiles were then removed under reduced pressure, and the remaining solid was washed with THF (1 mL). The volatiles were once again removed under reduced pressure. To the remaining solid was added dtbpy (10.1 mg, 0.038 mmol) and fluorobenzene (250 µL). The resulting solution changed to a pale peach color (**Figure S20**). The solution was then filtered and stored at -35 °C, wherein crystalline material was observed after 10 days. Crystalline material was collected in 46% yield. Analysis for ($^{(tBu2P)}$ONO)$NpCl_2$(dtbpy). **^{1}H NMR** (C_6D_6, 23 °C) δ 65.50 (s, 47 Hz), 54.43 (s, 26 Hz), 16.23 (s, 9 Hz), 15.08 (d, *J* = 6 Hz), 13.05 (d, *t*BuP, 18 H, *J* = 10 Hz), 10.27 (s, 9 Hz), 9.21 (d, *J* = 6 Hz), 2.42 (s, tBu_{bpy} 18H, 6Hz), -1.86 (d, *t*BuP, 18 H, *J* = 10 Hz), -6.69 (s, 21 Hz). **^{31}P NMR** (C_6D_6, 23 °C) δ 79.3. UV/vis/NIR (C_6H_6:C_6D_6 60:40, 1.6 mM, 25 °C, $L{\cdot}mol^{-1}{\cdot}cm^{-1}$): 511 nm (ε = 77.5), 640 nm (ε = 63.1), 740 nm (ε = 83.8), 816 nm (ε = 47.5), 900 nm (ε = 75.0), and 966 nm (ε = 73.8).

1.5 Synthesis of (1,3-iPr$_2$-4,7-Me$_2$-C_9H_3)($^{(tBu2P)}$ONO)UCl, 3. A 20 mL scintillation vial was charged with a stir bar, (50 mg, 0.13 mmol) of UCl_4, 2,6-pyridinedicarboxaldehyde (18 mg, 0.13 mmol) and THF (1 mL). The reaction was allowed to mix at room temperature for 20 min, where a tan slurry is formed. $^tBu_2PSiMe_3$ (60 mg, 0.27 mmol) was added to this tan slurry and the resulting bright green solution was allowed to mix at RT for 20 min prior to removing all volatiles under reduced pressure. During this time, to a second 20 mL was added 1,3-$(iPr_2)_2$-4,7-Me_2-C_9H_3 (30 mg, 0.13 mmol) and THF (5 mL) followed by KHMDS (26 mg, 0.13 mmol), resulting in an immediate color change from a clear to yellow solution. All volatiles were removed under reduced pressure after mixing 5 min at room temperature. The remaining solids from both the uranium solution and the deprotonated indene solution were dissolved in THF (1 mL). The deprotonated indene solution was added dropwise to the uranium solution, and the vial was washed 3 x 1 mL THF. The resulting solution, which turned dark red in color, was allowed to mix at RT for 3 hr. Volatiles were removed under reduced pressure, and the resulting red material was dissolved in pentane (5 mL). This solution was then filtered to remove any KCl salts. The remaining salt-free solution was then concentrated to approximately 1 mL under reduced pressure, and then stored at -35 °C. Crystalline material of **3** was isolated from this solution. $(^{(OTMS)}PNO^{tBu})UCl_2(\eta^5\text{-}C_9H_3\text{-}1,3\text{-}(iPr_2)_2\text{-}4,7\text{-}Me_2$ (**3b,** $^{(OTMS)}PNO^{tBu}$ = 2-((trimethylsiloxy)(*tert*-butylphosphino)-methyl-6-((*tert*-butylphosphino-methanolato)pyridine)) could be isolated from this reaction, though in limited quantities and is a likely contaminant of **3** (see SI Section 3 for more details). Further characterization of **3b** was not pursued. Crystallization of **3** from diethyl ether produced crystalline material of **3** that was collected in 61% yield. Analysis for $(1,3\text{-}(iPr_2)_2\text{-}4,7\text{-}Me_2\text{-}C_9H_3)(^{(tBu2P)}ONO)UCl$. Calculated: C = 51.86%, H = 6.96%, N = 1.51%. Found: C = 49.23%, H = 6.87%, N = 1.36%. **^{1}H NMR** (C_6D_6, 23 °C) δ 78.90 (s, 15Hz), 44.75 (s, 27 Hz), 32.21 (s, 27Hz, 18H, *t*BuP,), 27.02 (s, 17Hz, 6H, *i*Pr), 9.93 (s, 8Hz, 6H, *i*Pr), -1.61 (s, 11 Hz), -2.97 (d, 18H, *t*BuP, *J* = 6 Hz), -5.72 (d, *J* = 3 Hz, 6 Hz), -6.35 (s, 160 Hz), -18.98 (s, 4 Hz), -21.25 (s, 19 Hz), -64.31 (s, 17 Hz) **^{31}P NMR** (C_6D_6, 23 °C) δ 81.8. UV/vis/NIR (toluene, 10 mM, 25 °C, $L{\cdot}mol^{-1}{\cdot}cm^{-1}$): 507 nm (ε = 452.3), 636 nm (ε = 125.1), 670 nm (ε = 91.4), 1018 nm (ε = 36.4), 1085 nm (ε = 44.2), and 1139 nm (ε = 69.6).

1.6 Synthesis of $(1,3\text{-}iPr_2\text{-}4,7\text{-}Me_2\text{-}C_9H_3)(^{(tBu2P)}ONO)NpCl$, 4. $1,3\text{-}iPr_2\text{-}4,7\text{-}Me_2\text{-}C_9H_3$ (8.5 mg, 0.037 mmol) was deprotonated with KHMDS (7.5 mg, 0.038 mmol) in THF in an argon-filled, positive pressure dry box. The volatiles were then removed under reduced pressure. This vial was then transferred to a transuranic, helium-filled, negative pressure dry box. A 20 mL scintillation vial was charged with a stir bar, $(dme)_2NpCl_4$ (20.2 mg, 0.036 mmol), 2,6-pyridine dicarboxaldehyde (4.9 mg, 0.037 mmol), and THF (1 mL). The resulting pale pink solution was allowed to mix at room temperature for 5 min prior to the addition of $^tBu_2PSiMe_3$ (18.3 mg, 0.084 mmol). The resulting golden yellow solution was allowed to mix at room temperature for 5 min. All volatiles were then removed under reduced pressure. Vials containing both the Np material and the deprotonated indene were dissolved in THF (1 mL). The deprotonated indene solution was then added dropwise to the Np solution. The vial containing the indene solution was washed with THF (3 x 1 mL), and the washings were added to the Np solution. The addition of the deprotonated indene to the Np solution resulted in an immediate color change to a dark, almost indistinguishable, solution (**Figures S18-19, S22-23**). After 5 min of mixing at room temperature, all volatiles were removed under reduced pressure. The resulting material was dissolved in approximately 500 µL pentane. This solution was then filtered to remove any KCl. The resulting solution was stored at -35 °C until crystalline material was observed. Crystalline material was collected in 12% yield. Analysis of $(^{(tBu2P)}ONO)NpCl(\eta^5\text{-}C_9H_3\text{-}1,3\text{-}(iPr_2)_2\text{-}4,7\text{-}Me_2)$. **^{1}H NMR** ($C_6D_6$, 23 °C) δ 51.91 (s, 60 Hz), 24.67 (s, 43 Hz), 15.37 (s, 57 Hz), 13.96 (s, 13 Hz), 10.07 (s, 5 Hz), 9.35 (d, *J* = 7 Hz, 15 Hz), 8.80 (d, 18H, *J* = 8 Hz, *t*BuP), 6.56 (s, 6H, *i*Pr, 26 Hz), 4.61 (d, *J* = 5 Hz, 21 Hz), -2.42 (s, 10 Hz), -11.34 (s, 6 Hz). **^{31}P NMR** (C_6D_6, 23 °C) δ 72.7. UV/vis/NIR (C_6H_6:C_6D_6 60:40, 1.2 mM, 25 °C, $L{\cdot}mol^{-1}{\cdot}cm^{-1}$): 572 nm (ε = 391.7), 725 nm (ε = 162.5), 817 nm (ε = 97.5), 881 nm (ε = 130.8), 904 nm (ε = 152.5), and 985 nm (ε = 73.3).

2. Theoretical Descriptions

2.1 Tables

Table S1. Calculated and experimental An-Cl, An-N, and An-O bond lengths for **1** and **2**. Distances are given in Å. The optimized cartesian coordinates of these systems are detailed in **Table S16**.

	1			**2**		
	Exp.	**PBE/TZP**	**B3LYP/TZP**	**Exp.**	**PBE/TZP**	**B3LYP/TZP**
An – Cl	2.669	2.618	2.636	2.651	2.626	2.625
An – N1 (dtbpy)	2.625	2.600	2.644	2.604	2.608	2.618
An – N2 (dtbpy)	2.613	2.572	2.642	2.570	2.605	2.617
An – N (ONO)	2.479	2.496	2.489	2.463	2.500	2.496
An – O1 (ONO)	2.174	2.177	2.177	2.153	2.180	2.165
An – O2 (ONO)	2.159	2.169	2.173	2.147	2.171	2.162

Table S2. Calculated and experimental An-Cl, An-N, An-O, and An-Centroid bond lengths for **3** and **4**. Distances are given in Å. The optimized cartesian coordinates of these systems are detailed in **Table S17**.

	3			**4**		
	Exp.	**PBE/TZP**	**B3LYP/TZP**	**Exp.**	**PBE/TZP**	**B3LYP/TZP**
An – Cl	2.603	2.597	2.597	-	2.592	2.585
An – Centroid	2.477	2.487	2.476	-	2.481	2.458
An – N (ONO)	2.466	2.477	2.524	-	2.488	2.479
An – O1 (ONO)	2.132	2.154	2.149	-	2.163	2.147
An – O2 (ONO)	2.123	2.152	2.149	-	2.163	2.146

Table S3. Calculated and experimental An-Cl, An-N, and An-O, bond lengths for the truncated structures of **1** and **2 (model)**. Distances are given in Å. The optimized cartesian coordinates of these systems are detailed in **Table S18**.

	1	**1 model**	**2**	**2 model**
	Exp.	**B3LYP/TZP**	**Exp.**	**B3LYP/TZP**
An – Cl	2.669	2.649	2.651	2.628
An – N1 (dtbpy)	2.625	2.566	2.604	2.611
An – N2 (dtbpy)	2.613	2.589	2.570	2.607
An – N (ONO)	2.479	2.498	2.463	2.497
An – O1 (ONO)	2.174	2.155	2.153	2.160
An – O2 (ONO)	2.159	2.159	2.147	2.158

Experimentally, a small decrease of the An-ONO bond lengths was observed after replacing the dtbpy by the indenide ligand. These changes were more pronounced in the An-O bonds (range of 0.036 – 0.042 Å for uranium complexes **1** and **3**). The geometry optimization process was able to reproduce this shrinking in the uranium systems with predicted values of 0.024 – 0.028 Å. Since no crystallographic data is available for **4**, the optimized geometries (**2** and **4**) confirm the same conclusion for the neptunium complexes (**Table S1** and **Table S2**).

The origin of this decrease in bond length could come from either the difference in the steric bulk of the ligand or the difference in chemical bonding. To differentiate them, simplified structures (**1 model** and **2 model**) with fewer steric interactions but the same chemical bonding environment were modeled. The model removed the six methyl groups of the tert-butyl branches of the ONO ligand, thus reducing the steric interaction between this and the dtbpy ligand. By comparing the geometric data (Table S3) of the model complex and its parent compound, **1** vs. **1 model** and **2** vs. **2 model**, it reveals a decrease of the An – ONO, as well as the An – dtbpy bond distances, as the steric hindrance is decreased in the complexes. This confirms the steric factor is important in complexes **1** and **2**, preventing the systems from becoming more compacted in the parent complexes. However, by comparing the **1 model** vs. **2 model**, the An – ONO bonds are nearly identical, hence further concluding the impact on the bond length change from the steric factor of the coordinating ligands. Conversely, when the indenide ligand is employed, it coordinates preferentially trans to the ONO moiety (since the symmetry of the 5-member ring is appropriate to interact with the *f* orbitals of the An center), allowing a better arrangement of the ligands around the metal.

Despite the small changes in the bond lengths, no significant differences were found in terms of An-O and An-N bond orders between dtbpy and indenide complexes (**Tables S12-15, S19**). In fact, the uranium complexes are identical, while almost negligible differences were found in case of the neptunium complexes (**Figure 4**, **Table S12-S15**). This means that the bond order is not sensitive to this small perturbation in the bond lengths.

Table S4. SO-CAS(2,7)SCF/NEVPT2 states for **1**. The assignment was done in terms of J and the composition of each state shows the RS terms with higher contributions. The first band corresponds to the ground manifold (GM) and the first state of this manifold is the SO-GS (highlighted in gray). The other bands (corresponding to the excited manifolds) were labeled with capital letters from A to H.

Band	J	Composition	Energy (cm^{-1})	Energy (nm)
GM	4	**88% ^{3}H + 8% ^{1}G**	**0.00**	**-**
		86% ^{3}H + 7% ^{1}G	275.24	36331.9
		85% ^{3}H + 8% ^{1}G	537.17	18616.1
		85% ^{3}H + 10% ^{1}G	694.35	14402.0
		86% ^{3}H + 8% ^{1}G	903.44	11068.8
		84% ^{3}H + 9% ^{1}G	1310.15	7632.7
		82% ^{3}H + 8% ^{1}G	1580.97	6325.2
		85% ^{3}H + 9% ^{1}G	1872.48	5340.5
		86% ^{3}H + 9% ^{1}G	1955.64	5113.4
A	2	59% ^{3}F + 12% ^{1}D	4850.58	2061.6
		67% ^{3}F + 13% ^{1}D	5174.41	1932.6
		75% ^{3}F + 7% ^{1}D	5266.26	1898.9
		51% ^{3}F + 7% ^{1}D	5423.75	1843.7
		63% ^{3}F + 10% ^{1}D	5473.81	1826.9
B	5	92% ^{3}H	6243.39	1601.7
		78% ^{3}H	6251.92	1599.5
		90% ^{3}H	6461.53	1547.6
		92% ^{3}H	6495.23	1539.6
		84% ^{3}H	6841.29	1461.7
		71% ^{3}H	7068.38	1414.8
		73% ^{3}H	7317.50	1366.6
		95% ^{3}H	7434.65	1345.1
		84% ^{3}H	7533.98	1327.3
		88% ^{3}H	7567.87	1321.4
		78% ^{3}H	7596.96	1316.3
C	3	56% ^{3}F + 13% ^{1}G	9400.47	1063.8
		36% ^{3}F + 34% ^{1}G	9622.19	1039.3
		65% ^{3}F + 15% ^{1}G	9662.73	1034.9
		74% ^{3}F + 11% ^{1}G	9671.26	1034.0
		68% ^{3}F + 9% ^{1}G	9781.97	1022.3
		78% ^{3}F + 4% ^{1}G	9835.25	1016.8

		68% ^{3}F + 9% ^{1}G	9947.77	1005.3
D	4	57% ^{3}F + 16% ^{1}G	10007.25	999.3
		40% ^{3}F + 33% ^{1}G	10106.64	989.4
		42% ^{3}F + 33% ^{1}G	10108.15	989.3
		71% ^{3}F + 19% ^{1}G	10340.39	967.1
		63% ^{3}F + 25% ^{1}G	10382.18	963.2
		46% ^{3}F + 35% ^{1}G	10482.85	953.9
		47% ^{3}F + 30% ^{1}G	10746.56	930.5
		60% ^{3}F + 29% ^{1}G	10964.10	912.1
		62% ^{3}F + 27% ^{1}G	10978.05	910.9
E	6	72% ^{3}H	11299.58	885.0
		75% ^{3}H	11380.10	878.7
		81% ^{3}H	11513.15	868.6
		88% ^{3}H	11580.39	863.5
		86% ^{3}H	11890.21	841.0
		82% ^{3}H	12191.56	820.2
		76% ^{3}H	12448.15	803.3
		81% ^{3}H	12734.02	785.3
		76% ^{3}H	12767.03	783.3
		78% ^{3}H	13041.30	766.8
		75% ^{3}H	13086.32	764.2
		64% ^{3}H	13209.32	757.0
		67% ^{3}H	13222.82	756.3
F	4	44% ^{3}F + 41% ^{1}G	16425.56	608.8
		46% ^{3}F + 39% ^{1}G	16619.35	601.7
		36% ^{3}F + 42% ^{1}G	16666.29	600.0
		39% ^{3}F + 36% ^{1}G	16893.04	592.0
		10% ^{3}F + 21% ^{1}G	16955.97	589.8
		41% ^{3}F + 41% ^{1}G	17046.54	586.6
		24% ^{3}F + 19% ^{1}G	17113.03	584.4
		40% ^{3}F + 42% ^{1}G	17164.58	582.6
		22% ^{3}F + 19% ^{1}G	17278.75	578.7
G	2	41% ^{3}F + 44% ^{1}D	17729.82	564.0
		42% ^{3}F + 50% ^{1}D	17839.47	560.6
		59% ^{3}P + 15% ^{1}D	18017.28	555.0
		41% ^{3}P + 33% ^{1}D	18114.86	552.0
		35% ^{3}P + 27% ^{1}D	18406.05	543.3

H	0	70% ^{3}P + 7% ^{1}S	18529.97	539.7

Table S5. SO-CAS(6,11)SCF/NEVPT2 states for **3**. The assignment was done in terms of J and the composition of each state shows the RS terms with higher contributions. The first band corresponds to the ground manifold (GM) and the first state of this manifold is the SO-GS (highlighted in gray). The other bands (corresponding to the excited manifolds) were labeled with capital letters from A to H.

Band	J	CAS(6,11)SCF/NEVPT2			CAS(2,7)SCF/NEVPT2	
		Composition	**Energy (cm^{-1})**	**Energy (nm)**	**Energy (cm^{-1})**	**Energy (nm)**
GM	4	**84% ^{3}H + 7% ^{1}G**	0.00	**-**	0	-
		84% ^{3}H + 8% ^{1}G	94.59	105719.4	94.54	105775.333
		86% ^{3}H + 9% ^{1}G	695.80	14371.9	695.8	14371.946
		86% ^{3}H + 8% ^{1}G	1022.21	9782.7	1022.2	9782.72566
		84% ^{3}H + 6% ^{1}G	1100.28	9088.6	1100.3	9088.59563
		81% ^{3}H + 8% ^{1}G	1863.31	5366.8	1863.3	5366.7935
		81% ^{3}H + 10% ^{1}G	1864.44	5363.5	1864.4	5363.5408
		82% ^{3}H + 9% ^{1}G	1982.82	5043.3	1982.8	5043.32214
		83% ^{3}H + 9% ^{1}G	2011.06	4972.5	2011.1	4972.50206
A	2	41% ^{3}F + 8% ^{1}D	5101.07	1960.4	5101.1	1960.37302
		61% ^{3}F + 9% ^{1}D	5364.99	1863.9	5365	1863.93637
		63% ^{3}F + 9% ^{1}D	5480.46	1824.7	5480.5	1824.66435
		58% ^{3}F + 9% ^{1}D	5581.95	1791.5	5582	1791.48864
		71% ^{3}F + 10% ^{1}D	5717.96	1748.9	5718	1748.87547
B	5	93% ^{3}H	6059.42	1650.3	6059.4	1650.32297
		63% ^{3}H	6291.82	1589.4	6291.8	1589.36524
		81% ^{3}H	6741.21	1483.4	6741.2	1483.41322
		76% ^{3}H	6960.42	1436.7	6960.4	1436.69491
		77% ^{3}H	7038.71	1420.7	7038.7	1420.71488
		86% ^{3}H	7399.13	1351.5	7399.1	1351.51025
		89% ^{3}H	7453.32	1341.7	7453.3	1341.68397
		75% ^{3}H	7877.43	1269.4	7877.4	1269.44955
		92% ^{3}H	7936.89	1259.9	7936.9	1259.93935
		84% ^{3}H	7980.15	1253.1	7980.2	1253.10928
		94% ^{3}H	8027.53	1245.7	8027.5	1245.71319
C	3	59% ^{3}F + 16% ^{1}G	9742.77	1026.4	9742.8	1026.40214
		49% ^{3}F + 14% ^{1}G	9755.97	1025.0	9756	1025.0134
		64% ^{3}F + 11% ^{1}G	9934.17	1006.6	9934.2	1006.62662

		37% ^{3}F + 19% ^{1}G	10001.07	999.9	10001	999.893011
		74% ^{3}F + 11% ^{1}G	10063.57	993.7	10064	993.683156
		50% ^{3}F + 31% ^{1}G	10100.32	990.1	10100	990.067641
		35% ^{3}F + 31% ^{1}G	10140.43	986.2	10140	986.151475
D	4	38% ^{3}F + 17% ^{1}G	10235.2	977.0	10235	977.020478
		55% ^{3}F + 23% ^{1}G	10312.37	969.7	10312	969.709194
		64% ^{3}F + 8% ^{1}G	10383.13	963.1	10383	963.100722
		66% ^{3}F + 19% ^{1}G	10496.29	952.7	10496	952.717579
		58% ^{3}F + 26% ^{1}G	10529.99	949.7	10530	949.668518
		51% ^{3}F + 18% ^{1}G	10805.01	925.5	10805	925.496598
		50% ^{3}F + 25% ^{1}G	10842.25	922.3	10842	922.317785
		41% ^{3}F + 26% ^{1}G	10907.78	916.8	10908	916.776833
		61% ^{3}F + 26% ^{1}G	10924.74	915.4	10925	915.353592
E	6	61% ^{3}H	11378.29	878.9	11378	878.866684
		53% ^{3}H	11476.5	871.3	11477	871.345794
		61% ^{3}H	12022.47	831.8	12022	831.775833
		63% ^{3}H	12202.82	819.5	12203	819.48271
		61% ^{3}H	12363.14	808.9	12363	808.856003
		69% ^{3}H	12652.57	790.4	12653	790.353264
		71% ^{3}H	12695.36	787.7	12695	787.689361
		76% ^{3}H	12935.18	773.1	12935	773.085492
		77% ^{3}H	12959.52	771.6	12960	771.633517
		67% ^{3}H	13554.84	737.7	13555	737.743861
		77% ^{3}H	13706.34	729.6	13706	729.589373
		78% ^{3}H	13745.07	727.5	13745	727.533581
		87% ^{3}H	13866.6	721.2	13867	721.157313
F	4	52% ^{3}F + 34% ^{1}D	16789.42	595.6	16789	595.61319
		35% ^{3}F + 26% ^{1}G	16956.36	589.7	16956	589.749215
		16% ^{3}F + 12% ^{1}G	17025.02	587.4	17025	587.370822
		42% ^{3}F + 34% ^{1}G	17034.28	587.1	17034	587.051522
		20% ^{3}F + 18% ^{1}G	17049.74	586.5	17050	586.519208
		25% ^{3}F + 20% ^{1}G	17144.76	583.3	17145	583.268591
		20% ^{3}F + 18% ^{1}G	17467.12	572.5	17467	572.504225
		47% ^{3}F + 38% ^{1}G	17687.33	565.4	17687	565.376459
		24% ^{3}F + 27% ^{1}G	17831.44	560.8	17831	560.807203
G	2	16% ^{3}F + 40% ^{1}D	17853.45	560.1	17853	560.115832
		25% ^{3}F + 23% ^{1}D	17870.67	559.6	17871	559.57611

		43% ^{3}F + 46% ^{1}D	18066.71	553.5	18067	553.504207
		39% ^{3}F + 7% ^{1}D	18115.99	552.0	18116	551.998538
		26% ^{3}F + 51% ^{1}D	18528.3	539.7	18528	539.714923
H	0	78% ^{3}P + 9% ^{1}S	18588.62	538.0	18589	537.96355

Table S6. SO-CAS(3,7)SCF/NEVPT2 states for **2**. The assignment was done in terms of J and the composition of each state shows the RS terms with higher contributions. The first band corresponds to the ground manifold (GM) and the first state of this manifold is the SO-GS (highlighted in gray). The other bands (corresponding to the excited manifolds) were labeled with capital letters from A to F. Since Np^{4+} is a f^3 system, each SO state is doubly-degenerate (Kramers doublets).

Band	J	Composition	Energy (cm^{-1})	Energy (nm)
GM	9/2	76% ^{4}I + 12% ^{2}H	0.00	-
		77% ^{4}I + 9% ^{2}H	169.59	58965.7
		77% ^{4}I + 11% ^{2}H	399.84	25010.0
		72% ^{4}I + 13% ^{2}H	857.01	11668.5
		72% ^{4}I + 14% ^{2}H	1092.23	9155.6
A	11/2	83% ^{4}I	5739.48	1742.3
		86% ^{4}I	5866.96	1704.5
		88% ^{4}I	6010.55	1663.7
		83% ^{4}I	6292.55	1589.2
		84% ^{4}I	6459.14	1548.2
		85% ^{4}I	6556.55	1525.2
B	3/2	62% ^{4}F + 14% ^{2}D	9380.85	1066.0
		61% ^{4}F + 20% ^{2}D	9717.57	1029.1
C	13/2	81% ^{4}I	10597.39	943.6
		83% ^{4}I	10626.48	941.0
		84% ^{4}I	10890.89	918.2
		79% ^{4}I	11097.24	901.1
		81% ^{4}I	11282.67	886.3
		85% ^{4}I	11455.64	872.9
		85% ^{4}I	11528.67	867.4
D	9/2	24% ^{2}H + 19% ^{2}G	12515.19	799.0
		20% ^{2}H + 18% ^{2}G	12603.96	793.4
		28% ^{2}H + 25% ^{2}G	12724.76	785.9
		29% ^{2}H + 23% ^{2}G	12802.25	781.1
		23% ^{2}H + 24% ^{2}G	13022.11	767.9

		55% ^{4}F + 9% ^{4}G	13179.33	758.8
E	5/2	49% ^{4}F + 3% ^{4}G	13227.60	756.0
		43% ^{4}F + 3% ^{4}G	13393.05	746.7
F	5/2, 3/2, 7/2, 15/2, 7/2	-	14301.67	699.219042
		-	14702.65	680.149497
		-	14772.41	676.937615
		-	14869.53	672.516213
		-	14979.84	667.563873
		-	15107.55	661.920695
		-	15164.8	659.421819
		-	15328.23	652.391046
		-	15552.17	642.997087
		-	15662.47	638.4689
		-	15782.65	633.607157
		-	15835.85	631.478576
		-	15901.62	628.866744
		-	15940.19	627.345094
		-	16037.95	623.521086
		-	16171.39	618.376033
		-	16292.4	613.783114
		-	17732.86	563.924827
		-	17943.37	557.308911
		-	18181.07	550.022633
		-	18362.94	544.575106

Table S7. SO-CAS(7,11)SCF/NEVPT2 states for **4**. The assignment was done in terms of J and the composition of each state shows the RS terms with higher contributions. The first band corresponds to the ground manifold (GM) and the first state of this manifold is the SO-GS (highlighted in gray). The other bands (corresponding to the excited manifolds) were labeled with capital letters from A to F. Since Np^{4+} is a f^3 system, each SO state is doubly-degenerate (Kramers doublets).

Band	J	CAS(7,11)SCF/NEVPT2			CAS(3,7)SCF/NEVPT2	
		Composition	**Energy (cm^{-1})**	**Energy (nm)**	**Energy (cm^{-1})**	**Energy (nm)**
GM	9/2	74% ^{4}I + 11% ^{2}H	0.00	-	0	-
		74% ^{4}I + 9% ^{2}H	394.33	-	366.6	27277.68685
		74% ^{4}I + 12% ^{2}H	1246.4	8023.10655	1188.86	8411.419343
		72% ^{4}I + 11% ^{2}H	1455.42	6870.86889	1386.32	7213.341797

		71% ^{4}I + 14% ^{2}H	1693.34	5905.48856	1605.15	6229.947357
		85% ^{4}I	6053.69	1651.88505	6037.86	1656.215944
		87% ^{4}I	6219.37	1607.8799	6207.17	1611.040136
A	11/2	84% ^{4}I	6618.09	1511.00997	6581.8	1519.341214
		81% ^{4}I	6850.71	1459.70272	6807.37	1468.996103
		87% ^{4}I	7056.16	1417.20142	6986.13	1431.407661
		84% ^{4}I	7242.92	1380.65863	7133.34	1401.867849
B	3/2	65% ^{4}F + 17% ^{2}D	9303.34	1074.88278	9563.01	1045.695864
		62% ^{4}F + 18% ^{2}D	10064.49	993.592323	10232.65	977.2639541
		81% ^{4}I	10864.44	920.434003	10883.07	918.8583736
		82% ^{4}I	10933.54	914.616858	10955.7	912.7668702
		87% ^{4}I	11326.23	882.906316	11313.46	883.9028909
C	13/2	75% ^{4}I	11642.18	858.945661	11648.16	858.5046909
		82% ^{4}I	11893.08	840.825085	11857.31	843.3616056
		84% ^{4}I	12076.68	828.042144	12013.03	832.4294537
		84% ^{4}I	12219.44	818.368109	12146.16	823.3054727
		24% ^{2}H + 20% ^{2}G	12804.73	780.96141	12905.4	774.8694345
		18% ^{2}H + 19% ^{2}G	13014.48	768.374918	13169.56	759.3268112
D	9/2	24% ^{2}H + 23% ^{2}G	13179.58	758.74952	13246.32	754.9266513
		31% ^{2}H + 25% ^{2}G	13225.05	756.140809	13402.86	746.1094125
		21% ^{2}H + 22% ^{2}G	13362.7	748.351755	13470.77	742.3480618
		52% ^{4}F + 8% ^{4}G	13551.59	737.92079	13659.63	732.0842512
E	5/2	46% ^{4}F + 2% ^{4}G	13640.65	733.102895	13659.63	732.0842512
		41% ^{4}F + 2% ^{4}G	13829.62	723.085667	13723.87	728.6574414
		-	14626.52	683.689627	13925.36	718.1142893
		-	14708.43	679.882217	14727.56	678.999101
		-	14800.49	675.653306	14840.42	673.8353766
		-	14884.96	671.819071	15063	663.8783775
	5/2,	-	15028.42	665.405944	15135.66	660.6913739
	3/2,	-	15136.88	660.638124	15266.48	655.0298432
F	7/2,	-	15378.73	650.248753	15380.39	650.1785715
	15/2,	-	15402.69	649.237244	15508.46	644.8093492
	7/2	-	15655.78	638.74173	15541.08	643.4559246
		-	15807.74	632.601498	15782.02	633.6324501
		-	16138.68	619.629363	16019.15	624.2528474
		-	16227.72	616.229513	16189.04	617.7018526
		-	16370.27	610.863474	16369.99	610.8739223

-	16466.44	607.295809	16464.65	607.3618328
-	16656.44	600.368386	16511	605.6568348
-	16934.4	590.513983	16649.76	600.609258
-	17076.35	585.605238	16897.59	591.8003692
-	17668.18	565.989253	17073.72	585.6954431
-	17878.92	559.317901	18053.65	553.9046121
-	18319.55	545.864937	18329.12	545.5799296
-	18423.06	542.797993	18651.67	536.1450208

Table S8. TD-DFT assignment of electronic transitions in **1**. Level of theory: ZORA-PBE/TZP. The 5*f* ->6*d* transitions do not appear as pure contributions to independent peaks, but they are observed in the region between 250-500 nm.

Wavelength (nm)	Oscillator Strength	Transition
307	0.0470	LMCT (dtbpy)
322	0.0120	LMCT (dtbpy)
352	0.0119	LMCT (dtbpy)
480	0.0111	MLCT (dtbpy)
751	0.0097	MLCT (dtbpy)
821	0.0253	MLCT (dtbpy)
920	0.0091	$f \rightarrow f$
993	0.0003	$f \rightarrow f$
1237	0.0040	$f \rightarrow f$
1422	0.0015	$f \rightarrow f$

Table S9. TD-DFT assignment of electronic transitions in **2**. Level of theory: ZORA-PBE/TZP. The 5*f* ->6*d* transitions do not appear as pure contributions to independent peaks, but they are observed in the region between 250-500 nm.

Wavelength (nm)	Oscillator Strength	Transition
352	0.0102	$n \rightarrow \pi^*$ (ONO)
390	0.0032	LMCT (Cl)
404	0.0036	LMCT (dtbpy)
571	0.0029	MLCT (dtbpy)
580	0.0098	MLCT (dtbpy)

663	0.0062	MLCT (dtbpy)
963	0.0021	$f \rightarrow f$
1052	0.0041	$f \rightarrow f$
1310	0.0040	$f \rightarrow f$

Table S10. TD-DFT assignment of electronic transitions in **3**. Level of theory: ZORA-PBE/TZP. The 5*f* ->6*d* transitions do not appear as pure contributions to independent peaks, but they are observed in the region between 250-500 nm.

Wavelength (nm)	Oscillator Strength	Transition
334	0.0169	LMCT (ind)
357	0.0145	$n \rightarrow \pi^*$ (ONO)
378	0.0115	LMCT (ONO)
387	0.0107	LMCT (ONO)
453	0.0026	LMCT (ONO)
587	0.0049	LMCT (ONO)
822	0.0001	MLCT (ONO)
911	0.0001	$f \rightarrow f$

Table S11. TD-DFT assignment of electronic transitions in **4**. Level of theory: ZORA-PBE/TZP. The 5*f* ->6*d* transitions do not appear as pure contributions to independent peaks, but they are observed in the region between 250-500 nm.

Wavelength (nm)	Oscillator Strength	Transition
331	0.0313	$\pi \rightarrow \pi^*$ (ONO)
332	0.0118	LMCT (ind)
340	0.0073	LMCT (ONO)
359	0.0173	$n \rightarrow \pi^*$ (ONO)
426	0.0101	MLCT (ind)
469	0.0063	MLCT (ind)
572	0.0091	MLCT (ONO)
763	0.0097	LMCT (ONO)
1187	0.0006	$f \rightarrow f$
1382	0.0006	$f \rightarrow f$

Table S12. NLMO decomposition for **1** at ZORA-PBE/TZP level of theory. NLMO/NPA bond orders are also detailed. In case of the chlorine atoms, the three most important NLMOs are described. The natural spin density is 1.84.

NLMO	Type	Composition	BO /NLMO	BO
1a	U 5f	**97% U** [**100% f**]	-	-
1b	U 5f	**75% U** [**100% f**] + **15% lig(bpy)**	-	-
2a	U-Cl1	**92% Cl** [**100% p**] + **8% U** [**40% d** + **60% f**]	0.080	
2b	U-Cl1	**90% Cl** [**100% p**] + **10% U** [**44% d** + **56% f**]	0.095	0.31
2c	U-Cl1	**85% Cl** [**42% s** + **58% p**] + **14% U** [**23% s** + **38% d** + **39% f**]	0.138	
3a	U-Cl2	**90% Cl** [**100% p**] + **10% U** [**45% d** + **55% f**]	0.095	
3b	U-Cl2	**90% Cl** [**100% p**] + **10% U** [**48% d** + **52% f**]	0.092	0.33
3c	U-Cl2	**85% Cl** [**42% s** + **58% p**] + **14% U** [**16% s** + **33% d** + **51% f**]	0.134	
4a	U-O1	**94% O** [**55% s** + **45% p**] + **5% U** [**16% s** + **49% d** + **35% f**]	0.051	
4b	U-O1	**88% O** [**13% s** + **87% p**] + **9% U** [**26% d** + **71% f**]	0.091	0.23
4c	U-O1	**87% O** [**100% p**] + **9% U** [**27% d** + **72% f**]	0.092	
5a	U-O2	**94% O** [**54% s** + **46% p**] + **5% U** [**15% s** + **51% d** + **34% f**]	0.046	
5b	U-O2	**88% O** [**14% s** + **86% p**] + **9% U** [**24% d** + **71% f**]	0.089	0.22
5c	U-O2	**87% O** [**100% p**] + **9% U** [**29% d** + **71% f**]	0.093	
6a	U-N1	**88% N** [**25% s** + **75% p**] + **9% U** [**13% s** + **32% d** + **55% f**]	0.086	0.12
7a	U-$N2_{bpy}$	**89% N** [**27% s** + **73% p**] + **8% U** [**18% s** + **35% d** + **47% f**]	0.081	0.12
7b	U-$N3_{bpy}$	**89% N** [**27% s** + **73% p**] + **8% U** [**18% s** + **35% d** + **47% f**]	0.080	0.12

Table S13. NLMO decomposition for **2** at ZORA-PBE/TZP level of theory. NLMO/NPA bond orders are also detailed. In case of the chlorine atoms, the three most important NLMOs described. The natural spin density is 3.01.

NLMO	Type	Composition	BO /NLMO	BO
1a	Np	**99% Np** [**100% *f***]	-	-
1b	Np	**99% Np** [**100% *f***]	-	-
1c	Np	**96% Np** [**100% *f***]	-	-
2a	Np-Cl1	**93% Cl** [**100% p**] + **7% Np** [**73% d** + **27% *f***]	0.068	
2b	Np-Cl1	**92% Cl** [**99% p**] + **8% Np** [**54% d** + **44% *f***]	0.074	0.28
2c	Np-Cl1	**85% Cl** [**37% s + 63% p**] + **14% Np** [**17% s** + **30% d** + **53% *f***]	0.138	
3a	Np-Cl2	**94% Cl** [**100% p**] + **6% Np** [**60% d** + **40% *f***]	0.057	
3b	Np-Cl2	**90% Cl** [**99%p**] + **10% Np** [**43% d** + **57% *f***]	0.098	0.28
3c	Np-Cl2	**87% Cl** [**38% s** + **62% p**] + **13% Np** [**24% s** + **44% d** + **32% *f***]	0.122	
4a	Np-O1	**95% O** [**60% s** + **40% p**] + **4% Np** [**21% s** + **61% d** + **17% *f***]	0.039	
4b	Np-O1	**88% O** [**100% p**] + **7% Np** [**38% d** + **62% *f***]	0.072	0.23
4c	Np-O1	**85% O** [**8% s** + **92% p**] + **12% Np** [**14% d** + **83% *f***]	0.121	
5a	Np-O2	**95% O** [**60% s** + **40% p**] + **4% Np** [**22% s** + **62% d** + **16% *f***]	0.040	
5b	Np-O2	**88% O** [**100% p**] + **8% Np** [**32% d** + **67% *f***]	0.078	0.23
5c	Np-O1	**85% O** [**8% s** + **92% p**] + **12% Np** [**14% d** + **83% *f***]	0.117	
6a	Np-N1	**88% N** [**25% s** + **75% p**] + **9% Np** [**14% s** + **31% d** + **55% *f***]	0.090	0.12
7a	Np-$N2_{(bpy)}$	**89% N** [**27% s** + **73% p**] + **8% Np** [**18% s** + **36% d** + **46% *f***]	0.075	0.09
7b	σ Np-$N3_{(bpy)}$	**89% N** [**27% s** + **73% p**] + **8% Np** [**14% s** + **36% d** + **49% *f***]	0.078	0.09

Table S14. NLMO decomposition for **3** at ZORA-PBE/TZP level of theory. NLMO/NPA bond orders are also detailed. In case of the chlorine atoms, the three most important NLMOs described. The natural spin density is 2.01.

NLMO	Type	Composition	BO /NLMO	BO
1a	U 5f	**97% Np** [100% f]	-	-
1b	U 5f	**95% Np** [100% f]	-	-
1c				
2a	U-Cl1	**91% Cl** [100% p] + **9% U** [50% d + 50% f]	0.086	
2b	U-Cl1	**91% Cl** [100% p] + **9% U** [50% d + 50% f]	0.088	0.30
2c	U-Cl1	**88% Cl** [52% s + 48% p] + **12% U** [24% s + 43% d + 33% f]	0.122	
3a	U-O1	**93% O** [60% s + 40% p] + **6% U** [16% s + 40% d + 44% f]	0.056	
3b	U-O1	**90% O** [9% s + 91% p] + **7% U** [2% s + 36% d + 61% f]	0.073	0.22
3c	U-O1	**87% O** [100% p] + **9% U** [29% d + 71% f]	0.089	
4a	U-O2	**93% O** [60% s + 40% p] + **6% U** [15% s + 38% d + 47% f]	0.056	
4b	U-O2	**89% O** [9% s + 91% p] + **8% U** [2% s + 30% d + 67% f]	0.078	0.21
4c	U-O2	**87% O** [100% p] + **9% U** [32% d + 68% f]	0.090	
5a	U-N	**89% N** [25% s + 75% p] + **9% U** [18% s + 28% d + 54% f]	0.077	0.12
6a	U-Ind	**91% lig** + **9% U** [2% s + 28% d + 70% f]	-	-
6b	U-Ind	**91% lig** + **9% U** [4% s + 23% d + 73% f]	-	-
6c	U-Ind	**93% lig** + **7% U** [8% s + 28% d + 64% f]	-	-

Table S15. NLMO decomposition for **4** at ZORA-PBE/TZP level of theory. NLMO/NPA bond orders are also detailed. In case of the chlorine atoms, the three most important NLMOs described. The natural spin density is 3.14.

NLMO	Type	Composition	BO /NLMO	BO
1a	Np 5f	**99% Np** [100% f]	-	-
1b	Np 5f	**99% Np** [100% f]	-	-
1c	Np 5f	**98% Np** [100% f]	-	-
2a	Np-Cl1	**91% Cl** [100% p] + **9% Np** [45% d + 55% f]	0.088	
2b	Np-Cl1	**90% Cl** [36% s + 64% p] + **10% Np** [27% s + 50% d + 22% f]	0.095	0.29
2c	Np-Cl1	**89% Cl** [19% s + 81% p] + **10% Np** [11% s + 49% d + 40% f]	0.100	
3a	Np-O1	**95% O** [50% s + 50% p] + **4% Np** [15% s + 56% d + 29% f]	0.041	
3b	Np-O1	**89% O** [14% s + 86% p] + **7% Np** [5% s + 42% d + 52% f]	0.066	0.19
3c	Np-O1	**87% O** [5% s + 95% p] + **10% Np** [23% d + 75% f]	0.096	
4a	Np-O2	**95% O** [50% s + 50% p] + **4% Np** [16% s + 57% d + 27% f]	0.041	
4b	Np-O2	**89% O** [14% s + 86% p] + **7% Np** [4% s + 43% d + 53% f]	0.068	0.19
4c	Np-O2	**87% O** [5% s + 95% p] + **10% Np** [26% d + 73% f]	0.098	
5a	Np-N	**88% N** [25% s + 75% p] + **9% Np** [18% s + 23% d + 59% f]	0.090	0.12
6a	Np-Ind	**90% lig** + **10% Np** [3% s + 24% d + 73% f]	-	-
6b	Np-Ind	**91% lig** + **9% Np** [5% s + 21% d + 74% f]		
6c	Np-Ind	**84% lig** + **16% Np** [15% d + 83% f]	-	-

2.1.1 Raw Data For Figure 3

Energy and orbital compositions were obtained from fragment calculations performed at ZORA-B3LYP/TZP level of theory in AMS.2022.101. The orbital composition was normalized in terms of the most contributing fragments.

$(^{(tBu2P)}ONO)UCl_2(dtbpy)$ (**1**)

Energy	**Composition**
-0.941	94% dtbpy + 6% U (*d*)
-1.715	100% ONO
-1.894	100% ONO
-2.017	91% dtbpy + 9% U(*f*)
-2.198	90% dtbpy + 4% U(*f*) + 6% U(*d*)
-2.554	23% ONO + 77% U(*f*)
-2.639	7% ONO + 93% U(*f*)
-2.732	17% dtbpy + 83% U(*f*)
-2.836	15% dtbpy + 85% U(*f*)
-3.066	3% ONO + 97% U(*f*)
-3.238	52% dtbpy + 2% ONO + 46% U(*f*)
-3.415	3% dtbpy + 97% U(*f*)
-3.572	15% dtbpy + 85% U(*f*)
-5.179	95% ONO + 5% U(*d*)
-5.237	90% ONO + 3% U(*d*) + 7% U(*f*)
-5.857	94% dtbpy + 6% U(*d*)
-6.289	95% ONO + 5% U(*d*)
-6.385	96% Cl + 4% U(*f*)
-6.491	95% Cl + 5% U(*f*)
-6.585	90% ONO + 6% U(*d*) + 4% U(*f*)
-6.771	91% Cl + 4%U(d) + 5% U(*f*)
-6.837	94% dtbpy + 6% U(*d*)
-6.879	97% dtbpy + 3% U(*d*)
-6.923	100% ONO
-6.993	100% Cl

$((^{tBu2P})ONO)NpCl_2(dtbpy)$ (**2**)

Energy	Composition
-0.7001	100% dtbpy
-1.0162	100% dtbpy
-1.2967	100% dtbpy
-1.6739	100% ONO
-2.0478	93% ONO + 3% Np(*d*)+ 4% Np(*f*)
-2.2458	100% dtbpy
-2.5512	100% dtbpy
-2.8361	69% dtbpy + 5% Np(*d*) 26% Np(*f*)
-3.1729	8% ONO + 92% Np(*f*)
-3.2952	12% dtbpy + 88% Np(*f*)
-3.3444	5% dtbpy + 5% ONO + 90% Np(*f*)
-3.5025	28% dtbpy + 72% Np(*f*)
-3.919	5% ONO + 4% Np(*d*) + 91% Np(*f*)
-4.1088	5% ONO + 3% Np(*d*) + 92% Np(*f*)
-4.1368	2% dtbpy + 98% Np(*f*)
-5.0631	92% ONO + 3% Np(*d*)+ 5% Np(*f*)
-5.0999	90% ONO + 4% Np(*d*) + 6% Np(*f*)
-5.7141	95% dtbpy + 5% Np(*f*)
-6.0157	95% ONO + 5% Np(*f*)
-6.2492	92% Cl
-6.2984	97% Cl + 3% Np(*f*)
-6.3519	96% Cl + 4% Np(*f*)
-6.3716	100% ONO
-6.4302	91% ONO + 3% Np(*d*) + 6% Np(*f*)
-6.5227	87% Cl + 4% Np(*d*)+ 9% Np(*f*)
-6.563	87% Cl + 3% Np(*d*) + 10% Np(*f*)
-6.7678	100% dtbpy
-6.8292	100% Cl
-6.8346	100% ONO

$(^{(tBu2P)}ONO)U(1,3-{}^{i}Pr_2-4,7-Me_2-C_9H_3)Cl$ (**3**)

Energy	**Composition**
-0.7633	100% Ind
-0.9022	80 % Ind + 20% U(*d*)
-1.6215	86% Ind + 7% U(*d*) + 7% U(*f*)
-2.1076	100% ONO
-2.1932	89% ONO + 11% U(*f*)
-2.7072	3% ONO + 9% Ind + 88% U(*f*)
-2.8011	5% ONO + 8% Ind + 87% U(*f*)
-3.0902	8% ONO + 92% U(*f*)
-3.3304	5% ONO + 95% U(*f*)
-3.3777	7% ONO + 93% U(*f*)
-3.7354	5% Ind + 95% U(*f*)
-3.7805	4% Ind + 96% U(*f*)
-4.8331	86% Ind + 3% U(*d*) + 11% U(*f*)
-5.4122	90% ONO + 4% U(*d*) + 6% U(*f*)
-5.4489	88% ONO + 5% U(*d*) + 7% U(*f*)
-5.888	92% Ind + 8% U(*f*)
-6.1804	95% ONO + 5% U(*f*)
-6.5173	95% Ind + 5% U(*f*)
-6.7992	95% ONO + 5% U(*f*)
-6.816	95% Cl + 5% U(*f*)
-6.884	94% Cl + 6% U(*f*)
-6.9863	100% Cl

(${}^{(tBu2P)}$ONO)Np(1,3-${}^{i}Pr_2$-4,7-Me_2-C_9H_3)Cl (**4**)

Energy	Composition
-0.7908	100% Ind
-0.9447	85% Ind + 15% Np(*d*)
-1.7222	92% Ind + 8% Np(*d*)
-2.1171	100% ONO
-2.5054	91% ONO + 4% Np(*d*) + 5% Np(*f*)
-3.3511	4% ONO + 4% Ind + 92% Np(*f*)
-3.4845	21% Ind + 79% Np(*f*)
-3.581	5% Ind + 6% ONO + 89% Np(*f*)
-3.7481	3% ONO + 6% Ind + 91% Np(*f*)
-4.2943	4% Ind + 96% Np(*f*)
-4.3607	6% Ind + 94% Np(*f*)
-4.5304	100% Np(*f*)
-4.9614	77% Ind + 4% Np(*d*) + 19% Np(*f*)
-5.3778	94% ONO + 3% Np(*d*) + 3% Np(*f*)
-5.3924	94% ONO + 3% Np(*d*) + 3% Np(*f*)
-5.9745	96% Ind + 4% Np(*f*)
-6.1132	94% ONO + 6% Np(*f*)
-6.4632	95% ONO + 5% Np(*f*)
-6.5407	96% Ind + 4% Np(*f*)
-6.7302	94% ONO + 6% Np(*f*)
-6.7868	95% Cl + 5% Ind
-6.9124	92% Cl + 5% Ind + 3% Np(*f*)
-6.9373	95% Cl + 5% Np(*d*)

Table S16. Optimized Cartesian Coordinates for **1** and **2**. Level of theory: ZORA-B3LYP/TZP.

1	**2**
U 16.85505620382039 11.74836444154461 7.97486837104347	Np 10.22742892327810 12.32022812902987 6.83200726762001
P 14.73705188310940 12.64954589004166 12.30529069637341	Cl 10.67699841000155 14.89696214385044 6.62695262784232
Cl 16.35778932758612 9.16676416670276 8.20635126015179	P 12.32962177029744 11.41099401013955 2.50447607780474
P 12.99159638510317 12.30884058335773 5.02177926325197	Cl 9.02215044006880 10.01288659127084 7.18046744252701
C 13.53435228927713 10.67898960388795 10.83427178011905	P 14.09038201866010 11.77319470500027 9.77122794898185
H 12.73416428102317 11.42512783704878 10.75242355719354	O 10.62576773709543 11.88812692103474 4.74864148374990
H 13.07185282439651 9.68457658476536 10.78423030732484	O 11.52410044984937 12.03489707831929 8.53875633809815
H 14.20013401416581 10.77349522100068 9.97315041214326	N 12.25224120386688 10.92412774488409 6.40618969011418
O 15.53845600171717 11.98409149139683 6.26283055095427	N 8.42317048132561 13.02990789785862 8.58957115793821
C 14.49367734735688 12.88070985504571 6.04219050896542	N 7.85560523119115 13.01360044655002 5.96816528723733
H 14.85496185658923 13.73187087442163 5.43468971365542	C 12.47869347427117 10.46446189652574 5.16779049289799
C 12.71839542692053 10.50197560946320 5.51900717056153	C 5.58300694146285 13.67251358573995 6.29940124355881
C 12.63093351034399 10.51106191017900 7.05391246619254	H 4.79013336235679 13.92878569405643 6.99080392611468
H 13.61019067516804 10.67366463259373 7.51053473443124	C 14.09202802781767 9.68144509190881 7.26087554025283
H 12.26542898421883 9.53521942539784 7.39942135753274	H 14.72069951573214 9.41145736703044 8.10405602633620
H 11.93486379541670 11.27762654385589 7.41711700845601	C 6.84776921603195 13.33469898237485 6.79415781800708
C 13.77347198624398 9.48055031119125 5.08155975516870	C 14.32781573133794 9.18157995502963 5.98164382049303
H 13.81402011495341 9.37467065984040 3.99223183500355	H 15.15082457214238 8.48982568505267 5.81337623240140
H 13.51407220927337 8.49606088955970 5.49498141900706	C 13.52287368174829 9.57527363631885 4.91436749958643
H 14.76518973751878 9.74604148966615 5.45541450975423	H 13.70252006128935 9.22267461441884 3.90320026097190
C 13.69593835974682 12.43305972020185 3.26092774604823	C 11.47435033626267 10.96315970347973 4.14519537352265

C	12.77214094395596	11.67997334465359	2.29341747422232	H	10.89386891979547	10.06883547368106	3.84888816402882
H	12.85323730205688	10.59473182937194	2.40622054329838	C	7.15687291167639	13.31970944346528	8.25183274999370
H	13.05140238810342	11.92679899881106	1.25991482055797	C	6.51668949497387	13.57981425849647	10.58333755023810
H	11.72258709287984	11.96465776168281	2.43278313821148	C	13.02953176546558	10.56754830250566	7.43799145961330
C	14.05870379849512	13.49072848694265	7.36396039744282	C	12.59357372258695	11.17051892491946	8.76008747890470
C	13.00762953476349	14.39089743917619	7.53744358342859	H	12.25477611636389	10.31360020691201	9.37284086537282
H	12.38529609450929	14.66962990714407	6.69246880974234	C	14.32241044551400	13.58763319874225	9.28126207569821
C	12.77455119709611	14.89447008387711	8.81615375625550	C	8.75505967542310	13.01892244765793	9.88425713559684
H	11.95880508365370	15.59543900318097	8.98132981097977	H	9.79389283256061	12.77962692154921	10.10169443885854
C	13.57126842340534	14.49304872342091	9.88701026629482	C	6.19007297354918	13.59400187403581	9.22581851675788
H	13.39296744786663	14.85105068432640	10.89646650554934	H	5.17447682362207	13.81530729377359	8.92235622660238
C	14.60474245685840	13.58979519189483	9.63897411547311	C	9.51960510298355	11.60393874888844	1.70510591095617
N	14.82604553694323	13.12600964065782	8.40082888540597	H	9.19571892888895	11.11125102066409	2.62716994616353
C	15.60362861772717	13.08314320943134	10.66616923214169	H	8.78983964344059	11.35925198252818	0.91936969253133
H	16.19060860875831	13.97320563087617	10.96183978259366	H	9.49148248944501	12.68499964884126	1.86674678256294
C	16.15503689344134	12.92134236067842	13.54097219420479	C	5.49649733183227	13.86106085312972	11.68812745531642
C	17.54315494113647	12.43351689641499	13.11241502672670	C	5.33182375491831	13.68659229602012	4.92593825790223
H	17.56266913093494	11.35404758038778	12.93967408341927	C	12.74221056730429	13.25353537701574	2.65444086125430
H	18.27110812897198	12.66483438917535	13.90383299233687	C	7.63394930235279	13.02579359638072	4.65033433077768
H	17.87551658082268	12.93218360188429	12.19671679995953	H	8.48447702177975	12.75584275122338	4.02837515563073
C	15.77834683930817	12.28719822997889	14.88723869556349	C	10.91022423944012	11.12558279340173	1.27374841142879
H	14.77277887813559	12.58455308102443	15.20768372088843	C	14.39860279436737	13.58737296021959	7.74583051906117
H	16.48730664264773	12.62195744930926	15.65682900909727	H	15.10769885174834	12.83719673308306	7.37360523989100
H	15.82057694399485	11.19428489714154	14.85386480186024	H	14.73978858097548	14.57246381682597	7.40169324381963
C	14.30381665277795	10.81128319119198	12.15904601696871	H	13.41970017440168	13.40637755407877	7.29566541564250
C	15.46198567881349	9.80807914764243	12.16909143827327	C	6.40607363402271	13.35125182397794	4.09237386744598
H	16.17275960597811	10.01193963583682	11.36482732684539	H	6.30328320610659	13.33795522543714	3.01093705329313
H	15.06307431237279	8.79634242085057	12.01190076949274	C	3.96866703956514	14.04658134768236	4.33226057803365
H	15.99162491227345	9.80242254574418	13.12774055154480	C	13.50914458235367	13.39052360505286	3.98013870104463
O	16.44521515584484	12.14082602577313	10.07672851418348	H	12.84329214368251	13.28751559969797	4.84024464790152
N	18.69718460489107	11.04270156632015	6.21507665731612	H	13.96200394384938	14.38919974194063	4.03320085735870
C	19.96533460083746	10.75921898967690	6.55006287112140	H	14.31614716725160	12.65170891282181	4.06172475301722
C	20.27593015490927	10.75773019152258	8.00733435483249	C	11.57312945707179	14.24408079157301	2.64691201957011
N	19.26742186748022	11.08909829809460	8.82811290695877	H	11.04380024736132	14.24695577528702	1.68808664428108
C	19.48800841057870	11.08775679626528	10.14644537429260	H	11.96063704911401	15.25966100720941	2.80771471571344
H	18.63718347621853	11.36311607438206	10.76625762984493	H	10.86409237856955	14.03032653953037	3.45030617228403
C	20.71457548460355	10.76480808491964	10.70904799056109	C	11.27790931363285	11.75953434245295	-0.07517603430705
H	20.81610345630784	10.78756764485001	11.79042980113550	H	11.22799817348856	12.85224283589498	-0.04406865489856
C	21.78892773260038	10.41868474193893	9.87999458019256	H	10.56875571850944	11.41808643092248	-0.84166808101238
C	23.14955816310867	10.05828572679063	10.47909355704803	H	12.28453034375180	11.46862294833200	-0.39831862703244
C	24.18749184019903	9.72323983876850	9.40161974691062	C	14.31845001521019	12.39112331692982	12.50139550247673
H	23.88625984365666	8.85700329113043	8.80124785716721	H	15.37175428673201	12.12472564102915	12.35402771601161
H	25.14115119041780	9.47566646945063	9.87980663794647	H	14.05008424221839	12.13480320425158	13.53551058398624
H	24.36564264417258	10.57086786035234	8.72969545728447	H	14.21841589289389	13.47536818020168	12.39429727416128
C	22.98119763049967	8.83281838890941	11.39749313032143	C	13.72058152283256	13.59462782458899	1.51598794285699
H	22.27504240987810	9.02797290809932	12.21076173663461	H	14.58672283085272	12.92314100182127	1.52209178645570
H	23.94561485988035	8.56816873575214	11.84603095752831	H	14.08473793865559	14.62199055188351	1.65250393882982
H	22.61622341093342	7.96673657702193	10.83451642188035	H	13.25484279047766	13.53731072010806	0.52773141390559
C	21.53960042971974	10.42157604303306	8.50600643260354	C	3.45561683546375	12.85457345258978	3.50184606264945
H	22.33212420717594	10.15597449764871	7.81761260840144	H	4.13723163706894	12.60682649671618	2.68189204056721
C	20.93069188607533	10.47952958568861	5.57623120766683	H	2.48008645516751	13.09780131293990	3.06567753951034
H	21.94781245391299	10.26417510269323	5.87910189111053	H	3.33911308122903	11.96166637214199	4.12597929048919
C	20.60002182528573	10.48116192932980	4.21951527990037	C	5.97277519507704	15.06981899510474	12.51586729800024
C	21.61743172145114	10.19322412565121	3.11394149831195	H	6.94833476346643	14.88807428499534	12.97784955028132
C	18.36199045518885	11.04063814603963	4.92114654181913	H	5.25507564653822	15.27664109373618	13.31788517566697
H	17.32097318185242	11.27140422107391	4.70336709493599	H	6.05631321531315	15.96614798732337	11.89132999393539
C	19.26609243692554	10.76878176808880	3.90410372360075	C	5.39421392410921	12.62073905778998	12.59639168335505
H	18.91791307434709	10.78980555167844	2.87521758303701	H	5.06255236933879	11.74420066353506	12.02901836677145
C	16.21058116652335	14.44673136488880	13.74387305187574	H	4.66942896886879	12.80470297407800	13.39762431323143
H	16.46193158452047	14.98135696550616	12.82017911142316	H	6.35480373876022	12.37723750640858	13.06155536620752
H	16.98622884855496	14.69036194421093	14.48261176462286	C	4.13105302041008	15.27869942945119	3.42177144747117
H	15.25336408720946	14.83452958779816	14.10895228950347	H	4.49469564612424	16.14214346488573	3.98968383356967
C	23.01187695748180	9.88887808764991	3.67393216336391	H	3.16473224695202	15.54329980336637	2.97728553222013
H	23.41482455012644	10.73350507521088	4.24468007213233	H	4.83585961153674	15.09116473136819	2.60550676217464
H	23.70129729729570	9.69321321774782	2.84588956429368	C	13.24934370118875	14.58451655373853	9.73135717538076
H	23.00799925533248	9.00093705956724	4.31666427781458	H	12.26010545554357	14.29946877330247	9.36527603014591
C	23.66487072720248	11.25394661553556	11.30276909475200	H	13.48296758906873	15.57577367487062	9.31883776004753
H	23.78653953632745	12.14205665892993	10.67284297938308	H	13.21623057332079	14.68577528201746	10.82142148351945
H	24.63822869614118	11.00999929901859	11.74329505216010	C	4.10401625539830	14.17151652521372	11.12657949046240
H	22.98197742819912	11.50986021387843	12.11911238517417	H	4.11071493753462	15.06406455876368	10.49026221477154

C	21.14072358193616	8.97743733600223	2.29673955728768	H	3.41264730078624	14.36220248996881	11.95419555962635
H	21.05983259052314	8.08593497479517	2.92844742500488	H	3.70143955558586	13.33145385487195	10.54880209233018
H	21.85675287192364	8.76530083359108	1.49464391743085	C	7.84866819785698	13.28536786623352	10.90045983192114
H	20.16384631512721	9.15431562358166	1.83575019950815	H	8.19359535085404	13.25403078577834	11.93018012028285
C	21.71531562189937	11.42648739904622	2.19570987834281	C	11.94905720116389	12.07126333238862	11.74586018366003
H	20.75282376419393	11.66514688478045	1.73202481221031	H	11.80135167890035	13.12540360730818	11.49677376327973
H	22.43756209919629	11.23723522775167	1.39343226385230	H	11.67340204087840	11.92798461511853	12.80109157823015
H	22.04781904280995	12.30779813799716	2.75510788595177	H	11.26029621189342	11.47642659794648	11.13752646255532
Cl	18.04774050238775	14.06644105807818	7.60247334178757	C	13.40101407304552	11.62702583375994	11.53623036892822
C	11.33694725288029	10.08805342775069	4.98084693015451	C	2.93203587190885	14.37093865235237	5.41428882206330
H	10.55652412223885	10.78235981640872	5.31294004139411	H	2.75815053547146	13.51824960281059	6.08094064801529
H	11.08942047456634	9.08856346386113	5.36333869945100	H	1.97645211107221	14.61838711067146	4.93985106546872
H	11.30549904873727	10.04082466321502	3.88848611992031	H	3.23170495483523	15.23424048591557	6.01973039063771
C	15.14151814778759	11.96321343645605	3.06396012833839	C	10.86551859578806	9.59936771387061	1.07432390708560
H	15.83571515194892	12.55366628531717	3.67008874195135	H	11.82505414533717	9.21762352047696	0.70883037484088
H	15.42491094780268	12.09175445900056	2.00887955459264	H	10.09078776535030	9.34878596892690	0.33692566968053
H	15.27205950056280	10.90983794599207	3.32514969577130	H	10.61871599371451	9.06483503291294	1.99927221139259
C	13.32204088451796	10.48443622512366	13.29869304706203	C	13.51118131116155	10.12953655773229	11.87709077779151
H	13.78950708344667	10.53617168997092	14.28640047564378	H	12.89601417745217	9.50518243330647	11.21807976975352
H	12.94429077370205	9.46189178651976	13.16321313330105	H	13.16224869013037	9.95969878170793	12.90484464260861
H	12.46476747877708	11.16722973837536	13.29283833201755	H	14.54661677389751	9.77988764536468	11.80267995536995
C	13.61382472988839	13.93040281669264	2.91203938313263	C	15.69860692903697	14.02865802404324	9.81114380807464
H	12.58371523957148	14.29752302985544	2.97518626547050	H	15.73772853551624	14.07011246975606	10.90349237038628
H	13.97496331500252	14.08980003771059	1.88687125889154	H	15.92105638862291	15.03559348748778	9.43272351785176
H	14.23299183207200	14.54749432736824	3.57411908837225	H	16.49147377255939	13.35372680841232	9.46877748569863

Table S17. Optimized Cartesian Coordinates for **3** and **4**. Level of theory: ZORA-B3LYP/TZP.

3				**4**			
U	5.19413582272441	5.15373827590963	11.65393352774895	Np	5.22866773625421	5.09271084342000	11.71264676066301
Cl	4.27199281951165	6.20483331620019	9.46490376850933	Cl	4.30860764962636	6.11290808842258	9.52278146224769
P	1.36994268939166	2.19005912324781	12.37144311665533	P	8.17308048605366	1.94130770195778	9.42913558642080
P	8.19293723913686	2.02257606083167	9.39097435734300	P	1.34980174945021	2.21459904752517	12.39440798109904
O	6.89149658557946	4.14427754814718	10.80592204596537	O	6.90330347217531	4.09863553444622	10.81033146926241
O	3.37197837436717	4.23160302079082	12.32243583718663	O	3.36503082471938	4.24269099307664	12.35694287191637
C	6.91765512420523	7.10824806356526	12.55593818451306	N	5.23434629057670	2.62569377760281	11.95539001571321
C	4.77157343696990	7.18015759325796	13.47750967788283	C	7.14879256063625	3.86737346945046	7.46560811549473
N	5.24471066536810	2.64436653786542	11.91617446307788	H	6.93303696250859	4.57721752182339	8.26818354175498
C	6.86311208950681	6.13572713699070	13.61859274454162	H	6.39734376941686	4.01388843054271	6.67740128788478
C	8.11782203062355	7.56112447216884	11.74797672935500	H	8.12392635810165	4.10633380665621	7.02973952474608
H	8.77942993999033	6.70274318635413	11.59506998746335	C	6.41833015737087	0.56628010001401	11.83348687386122
C	8.90322529775105	8.62937168527760	12.52653494510861	H	7.30043293486911	0.01652600813064	11.51935058363379
H	8.29101660965394	9.52983779424785	12.65800684024560	C	7.43827719551783	1.45993067226225	6.80599077252648
H	9.81551573058511	8.91372785874126	11.98811655508931	H	8.45268974554756	1.61498306737095	6.42737771772856
H	9.18616030012443	8.27672747711237	13.52405455583068	H	6.74355725006090	1.62832651856154	5.97196953942410
C	7.74067827612511	8.09255198762188	10.36139125593326	H	7.34934064228876	0.41278088238896	7.11676979817794
H	7.17961399159300	7.35642217590555	9.77499318001472	C	7.39378895438571	2.79988663347631	10.94265256623066
H	8.64516643835089	8.35447179434597	9.80090985929435	H	8.24874627614478	2.78936824675571	11.64461608828330
H	7.12767874598392	8.99863179858571	10.43161512573822	C	6.32662905122470	1.93538648288383	11.58759784560095
C	5.65168440115513	7.73763697547309	12.52018158920271	C	7.08085278498588	2.41743713368959	7.95714965356098
H	5.37911351894137	8.52236289950291	11.82232120497826	C	1.06140648180988	2.63934010852050	10.57104674882145
C	5.52381912925151	6.18147873000750	14.19478718042557	C	5.64022575204455	2.10536193261421	8.38740203362778
C	5.16398978390210	5.28220366288832	15.25275198496331	H	5.54487206788818	1.09520201392370	8.80453364054336
C	3.81123068432072	5.28424578754340	15.91306734988123	H	4.98099732738293	2.16926314588763	7.51193825698432
H	3.79239585927029	4.56231996987976	16.73552846243167	H	5.27897387883282	2.82797570006626	9.12276814794297
H	3.01548482639579	5.01518383248262	15.20952457867926	C	5.34364954504864	-0.06628588969559	12.45667940736396
H	3.55721509312854	6.26829144924139	16.32278768710777	H	5.38797725707348	-1.13500678746712	12.65690890711791
C	6.12993356037541	4.39754130411545	15.68822526154076	C	4.17795324299086	2.02248361408689	12.52575518789134
H	5.88852251261450	3.71346406133393	16.50031984338380	C	4.20318799499420	0.65658660153845	12.80339970689819
C	7.42897877967798	4.35312582979407	15.12933251717940	H	3.33829697595251	0.17871161430762	13.25404338367355
H	8.14429686668445	3.63682925089888	15.53055382438821	C	2.33342540963543	2.19895187415952	9.83194977397561
C	7.82592385784820	5.19131123289304	14.10706312092840	H	3.16848109863085	2.87154695597629	10.04036582225138
C	9.23213718884477	5.09870975562554	13.57803668286806	H	2.14928788311780	2.22887051778071	8.75000482878690
H	9.80305191131584	4.36255113505029	14.15233856927464	H	2.62756803866552	1.17473956255986	10.09316456222269
H	9.75852776762088	6.05746891933634	13.64226395257530	C	3.03966747871754	2.97560204813450	12.83883932536991
H	9.25016949720053	4.79353943159559	12.52581869085922	H	2.96618343951947	2.99911749604078	13.94252951311610
C	3.38848792802013	7.72224667566436	13.78089723253832	C	10.52684505630242	2.43969601827411	8.00895860285819

H	2.77614394892845	6.91009623989294	14.18530175440952	H	10.52762146840985	1.35377539390072	7.85628973948698
C	3.47874255035390	8.82261007298304	14.85152363861885	H	11.57203949943184	2.77666964358721	8.02597342764430
H	3.98590478408100	8.46723454835674	15.75474668200688	H	10.04508980586658	2.91001182634185	7.14652885040180
H	2.47952324969642	9.17714737466080	15.13245079072271	C	-1.26009614555815	2.93266563611934	13.10267932725904
H	4.04900176824003	9.67825951951005	14.47017921469976	H	-1.52231307041877	3.39602319024612	12.14694015457309
C	2.66708816054007	8.25365975112592	12.53784033169255	H	-1.93734564541575	3.34397219037564	13.86329083655782
H	3.18845290817946	9.11725355191551	12.10877543448784	H	-1.45216540134315	1.85549410530437	13.03056058180205
H	1.65581122734997	8.58263574707033	12.80261043277318	C	9.83968660209875	4.35545616129108	9.47185876995938
H	2.58154418204195	7.49364716027798	11.75329854687803	H	9.34599955133909	4.84635992800486	8.63055796279566
C	7.40290506351730	2.85008425327397	10.91316538470482	H	10.87537465576191	4.72190173341129	9.51410351803164
C	6.34408341154356	1.96807856018841	11.54795657876859	H	9.32508512738081	4.67851328597815	10.38012746386961
C	4.20039900718452	2.02452792395960	12.48863326447424	C	10.68672143297258	2.22486788506079	10.47375288909288
C	3.05249836352953	2.96355003310140	12.80986907559186	H	10.28968322282084	2.47467260273399	11.46481433946579
H	2.98626700247483	2.99134051059282	13.91325827840939	H	11.70811138799611	2.62565220820591	10.42582837152002
C	1.07409095389579	2.60299689217447	10.54615512868699	H	10.74312453101078	1.13334265946299	10.39645478320868
C	2.34814829057774	2.17132281690005	9.80501986087321	C	9.84858587893310	2.82833444937717	9.33117622722670
H	2.16101322314371	2.19695121731432	8.72350479568418	C	0.76785919165828	4.10248717780555	10.22307228912938
H	2.65094585678839	1.15028138921006	10.06840515343429	H	-0.19437983152548	4.43430717761537	10.62556244318885
H	3.17924272396051	2.84983071708848	10.01040904447152	H	0.71531458677300	4.20746070852788	9.13048057834868
C	-0.07081086183126	1.69341002866717	10.06388487045325	H	1.55506529961321	4.76974130580629	10.58389986963629
H	-1.02698546281349	1.93074955225023	10.53878973820701	C	-0.09130613195918	1.74372916785777	10.08144278990209
H	0.15109363810088	0.63789774281867	10.25829339066883	H	0.11789519635828	0.68518308858387	10.27377761954879
H	-0.19762288811687	1.82165036017351	8.98039039442168	H	-0.21221418407996	1.87625878824956	8.99775163473238
C	0.76316186834616	4.06109804114019	10.19158510397107	H	-1.04688855339771	1.99032984030807	10.55290670007550
H	0.70860775127126	4.16067474082271	9.09863882748236	C	0.41184193117809	4.74579614518447	13.54389447807060
H	1.54150472794508	4.74020622843464	10.54912555326301	H	1.44091594786825	5.00248499889533	13.80800405148748
H	-0.20269656065649	4.38305090292733	10.59331417449414	H	-0.25720089339161	5.19138148538789	14.29396524286477
C	0.20494986539420	3.19880808974865	13.48108996106351	H	0.19857117143555	5.21898154102650	12.58314454747081
C	0.42128853101178	2.63991043361080	14.90017930671101	C	0.19209390639855	3.22847256439379	13.50762594111665
H	1.42908092066366	2.84050439542838	15.28243549178856	C	0.39971115914331	2.65898037378662	14.92356649141921
H	0.25461946331068	1.55749405589170	14.93430509683854	H	0.21862868310762	1.57865867057708	14.95161892026136
H	-0.28627262301081	3.11851459824261	15.59024980225689	H	-0.30183934143990	3.14300806435138	15.61611594533937
C	-1.24477814047665	2.88533278956822	13.08037314910501	H	1.40988906289069	2.84388398673778	15.30766733947697
H	-1.42581070311994	1.80578728404755	13.01619575325435	C	5.68965476777728	7.69763509761864	12.53656833186539
H	-1.51285648060473	3.33933435550271	12.12179381534840	H	5.41712351723170	8.47888517171558	11.83504076195186
H	-1.92493516386193	3.29515436646769	13.83907737124859	C	6.95197826185677	7.06204175574682	12.56748285512191
C	0.40842320671809	4.71879981824404	13.50744684291025	C	6.89362359079947	6.08433278295754	13.62387097382295
H	-0.26005152498781	5.16122385208268	14.25979811055329	C	7.85028044086623	5.12702822905691	14.10263141797881
H	0.18206923067435	5.18405974834976	12.54575790652187	C	3.83954996407651	5.24073766198700	15.92037672631003
H	1.43641726017204	4.98863092661594	13.76273341042332	H	3.03923439919964	4.99001901305169	15.21553359815337
C	4.24173345386717	0.65820806433563	12.76172487331449	H	3.59931021684486	6.22321830999248	16.34182482601413
H	3.38404424759233	0.16932917971552	13.21442215382837	H	3.81467561277314	4.50962817367119	16.73448006467196
C	5.38940456141086	-0.05034982818509	12.40880030730675	C	4.81022414247687	7.14668915797676	13.49646833374805
H	5.44750503100556	-1.11910370086302	12.60490196311352	C	7.44483121396687	4.27792854800858	15.11139058906313
C	6.45430389735013	0.59899113761294	11.78620029690977	H	8.15337302176162	3.54993979841340	15.50349338254289
H	7.34348472587120	0.06265334443898	11.46873539686528	C	3.42848061860940	7.69056861314598	13.79852590009979
C	7.09861825396628	2.50233804065685	7.92174390351755	H	2.81211693200925	6.87635458679864	14.19190681225928
C	7.15324532247028	3.95779574028389	7.44481886662670	C	6.14585647710346	4.32797467431767	15.67381243554588
H	6.40092723636778	4.10569824555109	6.65781734345118	H	5.90001729083381	3.63562054914442	16.47745905372102
H	8.12649926900144	4.20998548325879	7.01226771025834	C	9.25678753277114	5.03368599395256	13.57520931727511
H	6.93114799983901	4.65824080730636	8.25378378642750	H	9.27552989664897	4.73923380824430	12.52010259694230
C	7.46937103569325	1.56087914590968	6.76137584607085	H	9.82363240301049	4.28963487850815	14.14329735173582
H	6.77752852231714	1.73340149532997	5.92586827117109	H	9.78600883560110	5.99009748431817	13.65051107897113
H	7.38710492261019	0.50976524364713	7.06014373164622	C	5.55527427047017	6.13674151673355	14.20413221437060
H	8.48447333008285	1.72812536917685	6.38997898583711	C	8.14871168012181	7.50437196715673	11.74974192748191
C	5.66023938276412	2.16952412561607	8.34466234416571	H	8.80337361303027	6.64109964613559	11.59537903687701
H	5.28876436675705	2.87881353834596	9.08804271374472	C	5.18956686907586	5.22995451556275	15.25536817090272
H	5.57557861870290	1.15394923524043	8.75070580392274	C	2.71522870327068	8.23718068001547	12.55755975548509
H	5.00247387515522	2.23562379227876	7.46834965253502	H	3.23684945999973	9.10932632069692	12.14626058488975
C	9.85681919269390	2.93199675678442	9.30878072599204	H	1.70103953292116	8.55901839726125	12.81997049751194
C	9.82704193296057	4.45730085647008	9.46561156293449	H	2.63994628994930	7.48739746977787	11.76260025832878
H	9.30355801706652	4.76364160193104	10.37469990313550	C	7.76538749594625	8.03475123244748	10.36459000815372
H	9.33237885909386	4.95069675821765	8.62625986629410	H	7.19230036382519	7.30144708390851	9.78697911442008
H	10.85738248302408	4.83699551605914	9.51827782360841	H	8.66828198125245	8.28622361108525	9.79676249160921
C	10.54467551015661	2.56581788508866	7.98492353523897	H	7.16229618989021	8.94734451663144	10.43688342784151
H	10.05932661808284	3.03792040027242	7.12547620564272	C	3.51944734980840	8.78031056307944	14.88009304007615
H	10.56100814440147	1.48157414331956	7.82182725945753	H	4.02124186193623	8.41541058864425	15.78254734263968
H	11.58490252745527	2.91709695340765	8.00913738734451	H	2.52030722634248	9.13589592215444	15.15966186443185
H	8.25667662321497	2.84300814873843	11.61566829056252	H	4.09409846002839	9.63747872564856	14.50882338007411
C	10.69883542557404	2.32798452825553	10.44850840018729	C	8.94568748138230	8.56911710013430	12.52164214050153

H	10.29857742148569	2.56805537398312	11.44059595359153	H	8.33946832610662	9.47290139178707	12.65801201590822
H	11.71657205859068	2.73816275570179	10.40428832398277	H	9.85434189274389	8.84849066855676	11.97468004210517
H	10.76502002910873	1.23755446098728	10.36401585823828	H	9.23628893324026	8.21555832229305	13.51672524795485

Table S18. Optimized Cartesian Coordinates for the models of **1** and **2**. Level of theory: ZORA-B3LYP/TZP.

1				2			
U	16.95568546509300	12.15218128094997	7.96248463518448	Np	10.20309373181746	12.11050337775867	6.83106417855491
P	14.54329022105435	12.22610845416566	12.04921158498539	Cl	10.72283344689564	14.67597865138884	6.57778928945659
Cl	16.34983070470081	9.55532581790773	8.07992350516939	P	12.48030869643307	11.52341246688395	2.73759766021844
P	13.02418438586717	12.27743666418135	5.32348956402616	Cl	8.93159073218531	9.85037055875337	7.24262332320929
H	20.80797748098690	11.35334946482486	1.69877380527564	P	14.13059310548093	11.88386674259769	9.42580886523917
H	22.34713786631551	10.52910628442701	1.36507979895060	O	10.56829545128917	11.62591597737503	4.75846679524719
H	22.25320462582659	11.75316735641830	2.65741817642355	O	11.49415496898371	11.81079247038437	8.53429094072436
Cl	18.02848958352567	14.55941368353404	7.75519803244715	N	12.19939085130443	10.67103769049919	6.41205331276205
O	15.65892324213949	12.46856827091107	6.27061738906955	N	8.44723803339342	12.90805418313762	8.58549831373029
C	14.49042429131227	13.23432099279084	6.10097142133032	N	7.84937109483098	12.83741904304030	5.96680302779824
H	14.67867557228291	14.05901008857563	5.38588587063137	C	12.40819491259949	10.18974347467396	5.17928621649727
C	12.94007189577803	10.84378243247627	6.49423796681300	C	5.59699358984677	13.55641684824147	6.30532614152109
H	22.48173533848632	8.39816935048767	11.20046809979138	H	4.81939126876358	13.85587919334217	6.99670739813321
C	21.51931590752812	10.61217995775786	8.52433971235481	C	14.00845381550206	9.39102517264699	7.27750913692889
H	22.26459416526258	10.20722569032820	7.84441206417831	H	14.63161837546000	9.10855272507231	8.12134327646300
C	20.79581454121751	10.39781879960347	5.61728619940081	C	6.86445108082251	13.22003015667939	6.79445015137093
H	21.74824250939576	9.98058390467381	5.93468437433332	C	14.22604513071328	8.86822537603687	6.00322247041053
C	20.45732459224525	10.39023617971002	4.26303392936889	H	15.02871730937140	8.15180645899354	5.84137963128060
C	21.36579336131888	9.81422808331210	3.17458031902758	C	13.42791353386818	9.26987088727400	4.93283290996617
C	18.38364654721153	11.44375936336253	4.92609545797442	H	13.59402362022993	8.89254539904885	3.92775983872270
C	13.92145190776056	11.50089491186344	3.87928297008089	C	11.46432488646722	10.76136858008375	4.14627689869369
H	23.26945559639260	10.02297476389080	4.25288613201238	H	10.92581202824602	9.92479456106535	3.66480543571791
H	23.28741733351447	8.85083607382203	2.92229682547499	C	7.19645546542240	13.25979802140878	8.24803376595130
H	22.49369418026527	8.42541349356124	4.45072849473755	C	6.60524130728737	13.65473907050172	10.57368554846607
C	23.84271617107943	11.61160253749034	11.07123217629039	C	12.96950548007487	10.30682791021648	7.44604190775405
C	14.07055137352583	13.81152273798867	7.43180108699004	C	12.60036850152084	10.99766415775698	8.73865996894195
C	12.99811525179878	14.67858414223130	7.64740757364620	H	12.37679074222787	10.22444416018047	9.49601362864624
H	12.37978082456691	15.00668263616673	6.81152809272599	C	14.27197473392720	13.25128963245528	8.19742591938550
C	12.74189096574081	15.10723055690491	8.95266005619774	C	8.79408211895902	12.92133755735906	9.87642902477618
H	11.91218691862452	15.78870076222890	9.14833870152751	H	9.81889968520811	12.62089594299425	10.09088354159767
C	13.54127894746069	14.66141732983820	10.00808698033525	C	6.26259584963559	13.63613364699552	9.22011521328147
H	13.35124047837738	14.97605728158829	11.03460729766099	H	5.26046833397256	13.91441483041755	8.91860482072675
C	14.59583619889202	13.79193587755521	9.72190060866951	H	4.81296939964834	14.83611180422082	2.57770889281944
N	14.84524230361625	13.39490576791116	8.45598821834082	H	6.40400954215197	12.58450053933896	13.11223317479656
C	15.54539988847262	13.18681809758359	10.72847851888137	C	4.12040722783084	15.06179637461336	3.39492960296175
H	16.03639639827442	13.99655414447078	11.30367274302560	H	4.50155434361537	15.94025640755820	3.92727284211304
C	15.96048970772336	11.40742976704754	12.91967590028445	C	5.62107599252230	14.05095996743578	11.67638099617885
H	23.22157335929117	12.06784257458277	11.85437635239273	C	5.32123311833897	13.50789258659106	4.93728699527889
C	20.61373139572605	8.67699202309025	2.44650698821987	C	13.15469188943772	13.00252176832400	3.60680540280752
C	22.67586423537146	9.24880383251377	3.74436508768353	C	7.60404383140951	12.78540680636062	4.65390036987848
H	24.81164545872703	11.34542982048193	11.51923822351426	H	8.43801123899543	12.46088573659328	4.03327231365098
H	17.40138898924335	11.85959655628672	4.69278284012148	C	11.09231690752857	12.31271836157028	1.81285713437365
C	19.20755872115537	10.94853082107615	3.92983780865172	H	3.15197480818219	15.32264840672782	2.95276091397346
H	18.86215785211155	10.99389650970524	2.89688875755503	C	4.24236889855805	14.42304624341612	11.11829266690301
H	24.01908460243980	12.36756938245163	10.29246013296268	H	4.29558662523153	15.28223140861589	10.43950365267907
C	13.93289254952234	10.81039635939892	11.02153958655733	H	3.57839692380341	14.69749596647776	11.94478134785712
H	20.36024956896611	7.86469714632105	3.14301090110704	C	6.37314047798848	13.11013507988388	4.10233567498023
H	21.24859255184921	8.26207802801495	1.64964082099477	H	6.24844110013688	13.04514494014571	3.02521312617231
H	19.68232972661430	9.03315397576615	1.98511049577530	C	3.95409560451789	13.86490135612975	4.35066057082854
C	21.70978073283858	10.93332213541197	2.16550975693319	H	3.29278326844596	11.78320368398140	4.22630153817101
O	16.50919508308349	12.41341479638995	10.05910993991121	C	6.18561880228282	15.26470061195806	12.43920919697446
N	18.71590180665991	11.44266958625508	6.23560915028693	H	7.15645259604416	15.04395176965613	12.89415968666755
C	19.92998894087231	10.93377061072754	6.58237793387168	C	13.30701270319577	12.78947397872190	10.80608158505564
C	20.27219889259523	11.00614449855595	8.01636320521701	H	3.77761466030394	13.58423066393257	10.58715374828873
N	19.31011100887395	11.51478492414167	8.83105224679476	C	7.91831045380818	13.28324746304282	10.88984322192842
C	19.59516458955300	11.64448590902471	10.14326690291157	H	8.27158100238231	13.26891797902229	11.91698916482702
H	18.79097090930626	12.05267371264929	10.75874307518957	H	5.49667125144064	15.55293142700767	13.24147519717810
C	20.81379500792890	11.28538638463560	10.69771108495170	H	3.25565405495790	15.12381664336031	6.00316924277893
H	20.96390176738135	11.43027249496636	11.76752834209171	C	3.41102985638252	12.65256313020222	3.57008676715684
C	21.82383356415205	10.74416126546164	9.88097774584409	H	4.07406765544829	12.36693032233844	2.74728992568462

C	23.17781210588342	10.34925265210155	10.47609196730082	H	2.43154505737174	12.89485856289973	3.14240484322065
C	24.12333348619561	9.74353933040687	9.42723117589835	H	6.31327228894663	16.12421097427264	11.77177781692122
H	23.70444362747044	8.83081801232403	8.97776812069499	C	5.45443866749346	12.86437534709482	12.64489635526757
H	25.07267838297082	9.47005612113615	9.90900489436230	H	5.06232575936069	11.98373571054026	12.12433694611716
H	24.35508309518862	10.45720953375775	8.62280161550646	H	4.75273959000240	13.13137968180682	13.44345787688976
C	22.95579431680763	9.30808034148603	11.59624747237490	C	2.93791402284404	14.24164375693192	5.43537257249267
H	22.32016601089192	9.70141082995811	12.40146543159215	H	2.76553142314358	13.41661206924071	6.13632164871389
H	23.92336589922562	9.02763768827697	12.03796350985201	H	1.97780709607632	14.48194261582978	4.96639225048842
H	13.92899468848520	10.40560671658245	6.69015957966266	H	14.98718845519923	13.98874599802499	8.57785249840418
H	12.28148869163338	10.08260113816514	6.05267311089141	H	13.31070773794512	13.74365703452018	8.01126667854142
H	12.48836478143802	11.16918691389302	7.44186133741893	H	14.66802514805334	12.86044924709145	7.25384843118486
H	14.90274641961478	11.97345744227273	3.74017036947503	H	13.95567962489727	12.69640576986682	4.28834631336749
H	13.33068175714562	11.63025992951587	2.96328105697065	H	12.38409040922628	13.54045373165808	4.17069146370890
H	14.08097871013256	10.42886339013756	4.05428306722706	H	13.59247819072171	13.67547082276552	2.86161604295153
H	16.63010184443446	10.90189403419069	12.21017570270644	H	11.50873703574172	12.94678793345213	1.02304536648353
H	15.55373521678683	10.67257945828858	13.62847994558395	H	10.47051371365932	12.92189899422721	2.47761391649798
H	16.52429035614327	12.15738737049604	13.49209238243581	H	10.47809413429893	11.54049361086434	1.33739946665459
H	14.72709718500223	10.36966972883900	10.40204563929704	H	13.02175912927480	12.08239897755851	11.59250693924866
H	13.11065892742640	11.15078813044407	10.37687123998693	H	12.42042898869961	13.32706865587196	10.45334684215137
H	13.53065757922561	10.04427961727656	11.69960679760521	H	14.01809326971343	13.50296085299142	11.23574214555613

Table S19. NLMO/NPA bond orders for complexes **1 – 4**.

Bond	**NLMO/NPA Bond Orders**			
	1	**2**	**3**	**4**
An – O1	0.21	0.22	0.21	0.20
An – O2	0.22	0.23	0.22	0.20
An – N_{ONO}	0.12	0.12	0.11	0.12
An – $N1_{dtbpy}$	0.11	0.10	-	-
An – $N2_{dtbpy}$	0.11	0.10	-	-
An – C_A	-	-	0.21	0.20
An – C_B	-	-	0.24	0.25
An – C_C	-	-	0.26	0.32
An – C_D	-	-	0.22	0.21
An – C_E	-	-	0.21	0.22

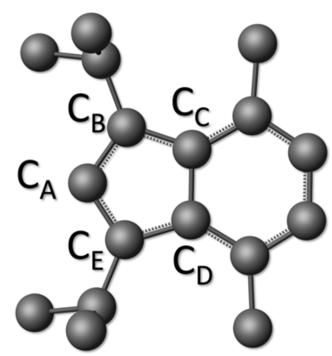

Table S20. Second-Order Perturbation Stabilization Energies [*E*(2), kcal/mol] of Donor (D) – Acceptor (A) interactions in **1**. The total stabilization for each ligand is specified, along with the most important contributions (over 5 kcal/mol). LP = Lone pair.

Ligand	Total Stabilization Energy (kcal/mol)	Most important interactions		
		D→A	Composition of An Orbital	E(2)
Cl	255	Cl1 (LP1) → An	*s*(30%), *f*(34%), *d*(36%)	7.74
		Cl1 (LP2) → An	*f*(81%), *d*(19%)	11.68
		Cl1(LP3) → An	*s*(22%), *f*(14%), *d*(64%)	5.01
		Cl1 (*σ*) → An	*f*(92%), *d*(8%)	11.23
		Cl1 (*σ*) → An	*s*(30%), *f*(34%), *d*(36%)	40.69
		Cl2 (LP1) → An	*s*(30%), *f*(34%), *d*(36%)	6.15
		Cl2 (LP2) → An	*s*(22%), *f*(14%), *d*(64%)	5.84
		Cl2 (LP3)→ An	*f*(13%), *d*(87%)	8.86
		Cl2 (*σ*) → An	*f*(92%), *d*(8%)	19.86
		Cl2 (*σ*) → An	*s*(30%), *f*(34%), *d*(36%)	31.39
		Cl2 (*σ*) → An	*s*(1%), *f*(51%), *d*(48%)	6.75
ONO	228	N → An	*s*(2%), *f*(67%), *d*(31%)	6.33
		N → An	*s*(1%), *f*(51%), *d*(48%)	16.28
		N → An	*s*(22%), *f*(14%), *d*(64%)	5.41
		O1 (LP1) → An	*s*(2%), *f*(67%), *d*(31%)	6.74
		O1 (LP1) → An	*f*(13%), *d*(87%)	5.45
		O1 (LP1) → An	*s*(42%), *f*(9%), *d*(49%)	9.84
		O1 (LP2) → An	*f*(81%), *d*(19%)	7.76
		O1 (LP2) → An	*s*(2%), *f*(67%), *d*(31%)	8.97
		O1 (LP2) → An	*s*(42%), *f*(9%), *d*(49%)	6.97
		O1 (LP3) → An	*f*(77%), *d*(23%)	7.09
		O2 (LP1) → An	*s*(2%), *f*(67%), *d*(31%)	6.82
		O2 (LP1) → An	*s*(42%), f(9%), *d*(49%)	9.20
		O2 (LP1) → An	*f*(21%), *d*(79%)	6.96
		O2 (LP2) → An	*f*(81%), *d*(19%)	6.67
		O2 (LP2) → An	*s*(2%), f(67%), *d*(31%)	10.43
		O2 (LP2) → An	*s*(42%), *f*(9%), *d*(49%)	7.25
		O2 (LP3) → An	*f*(77%), *d*(23%)	8.42
dtbpy	99	N1 → An	*f*(77%), *d*(23%)	6.98
		N1 → An	*f*(13%), *d*(87%)	5.09
		N1 → An	*s*(42%), *f*(9%), *d*(49%)	6.78
		N2 → An	*f*(77%), *d*(23%)	7.71
		N2 → An	*s*(42%), *f*(9%), *d*(49%)	6.74
		N2 → An	*f*(21%), *d*(79%)	5.02

Table S21. Second-Order Perturbation Stabilization Energies [$E(2)$, kcal/mol] of Donor (D) – Acceptor (A) interactions in **2**. The total stabilization for each ligand is specified, along with the most important contributions (over 5 kcal/mol). LP = Lone pair, LV = Lone vacant.

Ligand	Total Stabilization Energy (kcal/mol)	Most important interactions		
		D→A	Composition of An Orbital	E(2)
Cl	241	Cl1 (LP2) → An	*f*(1%), *d*(99%)	8.05
		Cl1 (σ) → An	*f*(92%), *d*(8%)	22.20
		Cl1 (σ) → An	*s*(7%), *f*(86%), *d*(7%)	7.83
		Cl1 (σ) → An	*s*(26%), *f*(34%), *d*(40%)	22.50
		Cl1 (σ) → An	*s*(2%), *f*(40%), *d*(58%)	11.75
		Cl2 (LP1) → An	*s*(26%), *f*(34%), *d*(40%)	6.10
		Cl2 (LP2) → An	*f*(1%), *d*(99%)	8.10
		Cl2 (LP3) → An	*s*(7%), *f*(86%), *d*(7%)	5.48
		Cl2 (σ) → An	*s*(7%), *f*(86%), *d*(7%)	11.67
		Cl2 (σ) → An	*s*(26%), *f*(34%), *d*(40%)	28.52
		Cl2 (σ) → An	*s*(2%), *f*(40%), *d*(58%)	12.62
ONO	238	N → An	*s*(26%), *f*(34%), *d*(40%)	8.10
		N → An	*s*(2%), *f*(40%), *d*(58%)	7.22
		N → An	*s*(31%), *f*(5%), *d*(64%)	8.93
		O1 (LP1) → An	*s*(7%), *f*(86%), *d*(7%)	8.21
		O1 (LP1) → An	*s*(30%), *f*(19%), *d*(51%)	9.95
		O1 (LP1) → An	*f*(26%), *d*(74%)	8.32
		O1 (LP3) → An	*s*(7%), *f*(86%), *d*(7%)	9.36
		O1 (LP3) → An	*f*(97%), *d*(3%)	5.89
		O2 (LP1) → An	*s*(7%), *f*(86%), *d*(7%)	8.47
		O2 (LP1) → An	*s*(30%), *f*(19%), *d*(51%)	5.12
		O2 (LP1) → An	*s*(1%), *f*(3%), *d*(96%)	6.56
		O2 (LP1) → An	*f*(26%), *d*(74%)	8.20
		O2 (LP3) → An	*s*(7%), *f*(86%), *d*(7%)	11.73
		O2 (LP3) → An	*f*(97%), *d*(3%)	5.11
		O2 (LP3) → An	*s*(1%), *f*(3%), *d*(96%)	6.90
dtbpy	85	N1 → An	*s*(31%), *f*(5%), *d*(64%)	5.35
		N1 → An	*s*(30%), *f*(19%), *d*(51%)	7.49
		N1 → An	*s*(1%), *f*(3%), *d*(96%)	6.21
		N2 → An	*s*(31%), *f*(5%), *d*(64%)	6.11
		N2 → An	*f*(97%), *d*(3%)	5.00
		N2 → An	*s*(1%), *f*(3%), *d*(96%)	9.88

Table S22. Second-Order Perturbation Stabilization Energies [*E*(2), kcal/mol] of Donor (D) – Acceptor (A) interactions in **3**. The total stabilization for each ligand is specified, along with the most important contributions (over 5 kcal/mol). LP = Lone pair, LV = Lone vacant.

Ligand	Total Stabilization Energy (kcal/mol)	Most important interactions		
		D→A	Composition of An Orbital	E(2)
Cl	138	Cl1 (LP2) → An	*f*(44%), *d*(56%)	15.65
		Cl1 (LP3) → An	*s*(41%), *f*(33%), *d*(26%)	12.80
		Cl1 (LP3) → An	*f*(7%), *d*(93%)	7.53
		Cl1 (σ)→ An	*s*(9%), *f*(72%), *d*(19%)	23.79
		Cl1 (σ)→ An	*s*(41%), *f*(33%), *d*(26%)	33.56
ONO	256	N → An	*s*(2%), *f*(88%), *d*(10%)	5.01
		N → An	*f*(7%), *d*(93%)	7.76
		N → An	*s*(30%), *f*(5%), *d*(65%)	6.30
		O1 (LP1) → An	*s*(2%), *f*(88%), *d*(10%)	11.52
		O1 (LP1) → An	*s*(30%), *f*(5%), *d*(65%)	5.60
		O1 (LP1) → An	*s*(10%), *f*(11%), *d*(79%)	12.43
		O1 (LP2) → An	*s*(2%), *f*(88%), *d*(10%)	7.10
		O1 (LP2) → An	*f*(44%), *d*(56%)	6.20
		O1 (LP3) → An	*s*(2%), *f*(88%), *d*(10%)	7.96
		O2 (LP1) → An	*s*(2%), *f*(88%), *d*(10%)	11.06
		O2 (LP1) → An	*s*(2%), *f*(6%), *d*(92%)	5.29
		O2 (LP1) → An	*s*(10%), *f*(11%), *d*(79%)	11.78
		O2 (LP2) → An	*s*(2%), *f*(88%), *d*(10%)	8.35
		O2 (LP2) → An	*f*(44%), *d*(56%)	6.31
		O2 (LP3) → An	*s*(2%), *f*(88%), *d*(10%)	6.76
		O2 (LP3) → An	*s*(2%), *f*(6%), *d*(92%)	8.11
ind	131	C_{A-E} → An	*f*(96%), *d*(4%)	10.98
		C_{B-C} → An	*s*(9%), *f*(72%), *d*(19%)	5.55
		C_{D-E} → An	*s*(30%), *f*(5%), *d*(65%)	6.92

Table S23. Second-Order Perturbation Stabilization Energies [*E*(2), kcal/mol] of Donor (D) – Acceptor (A) interactions in **4**. The total stabilization for each ligand is specified, along with the most important contributions (over 5 kcal/mol). LP = Lone pair, LV = Lone vacant.

Ligand	Total Stabilization Energy (kcal/mol)	Most important interactions		
		D→A	Composition of An Orbital	E(2)
Cl	119	Cl1(σ)→ An	*f*(60%), *d*(40%)	14.89
		Cl1 (LP2) → An	*s*(56%), *f*(10%), *d*(34%)	38.45
		Cl1 (LP3) → An	*s*(2%), *f*(90%), *d*(8%)	6.58
		Cl1 (LP3) → An	*s*(1%), *f*(93%), *d*(6%)	6.02
		Cl1 (LP3) → An	*s*(56%), *f*(10%), *d*(34%)	7.77

		Cl1 (LP3) → An	*f*(4%), *d*(96%)	6.41
ONO	269	N → An	*s*(2%), *f*(90%), *d*(8%)	6.72
		N → An	*f*(4%), *d*(96%)	6.81
		N → An	*s*(33%), *f*(3%), *d*(64%)	5.82
		O1 (LP1) → An	*s*(1%), *f*(93%), *d*(6%)	5.93
		O1 (LP1) → An	*s*(5%), *f*(9%), *d*(86%)	9.77
		O1 (LP2) → An	*s*(1%), *f*(93%), *d*(6%)	12.64
		O1 (LP2) → An	*f*(60%), *d*(40%)	9.49
		O1 (LP3) → An	*f*(5%), *d*(95%)	5.51
		O1 (LP1) → An	*s*(1%), *f*(93%), *d*(6%)	5.90
		O1 (LP1) → An	*s*(5%), *f*(9%), *d*(86%)	9.78
		O1 (LP2) → An	*s*(1%), *f*(93%), *d*(6%)	12.33
		O1 (LP2) → An	*f*(60%), *d*(40%)	9.03
		O1 (LP3) → An	*f*(5%), *d*(95%)	6.54
ind	133	$C_{A\text{-}E}$ → An	*s*(2%), *f*(90%), *d*(8%)	19.31
		$C_{B\text{-}C}$ → An	*f*(4%), *d*(96%)	5.83
		$C_{D\text{-}E}$ → An	*s*(33%), *f*(3%), *d*(64%)	5.13

2.2 Figures

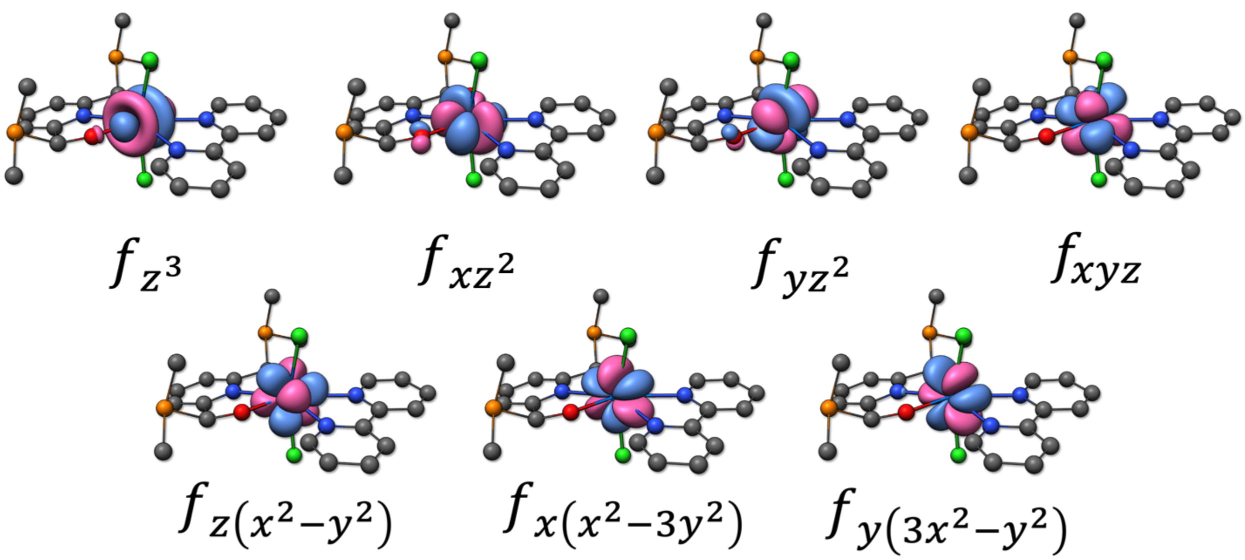

Figure S1. Active orbitals for **1** and **2**. The active space consisted of n electrons in 7 orbitals (n = 2,3 for U, Np). Since the keyword "*actorbs forbs*" was employed in the calculation of this minimum active space, all the orbitals are > 99% *f* in nature. Isovalue = 0.03.

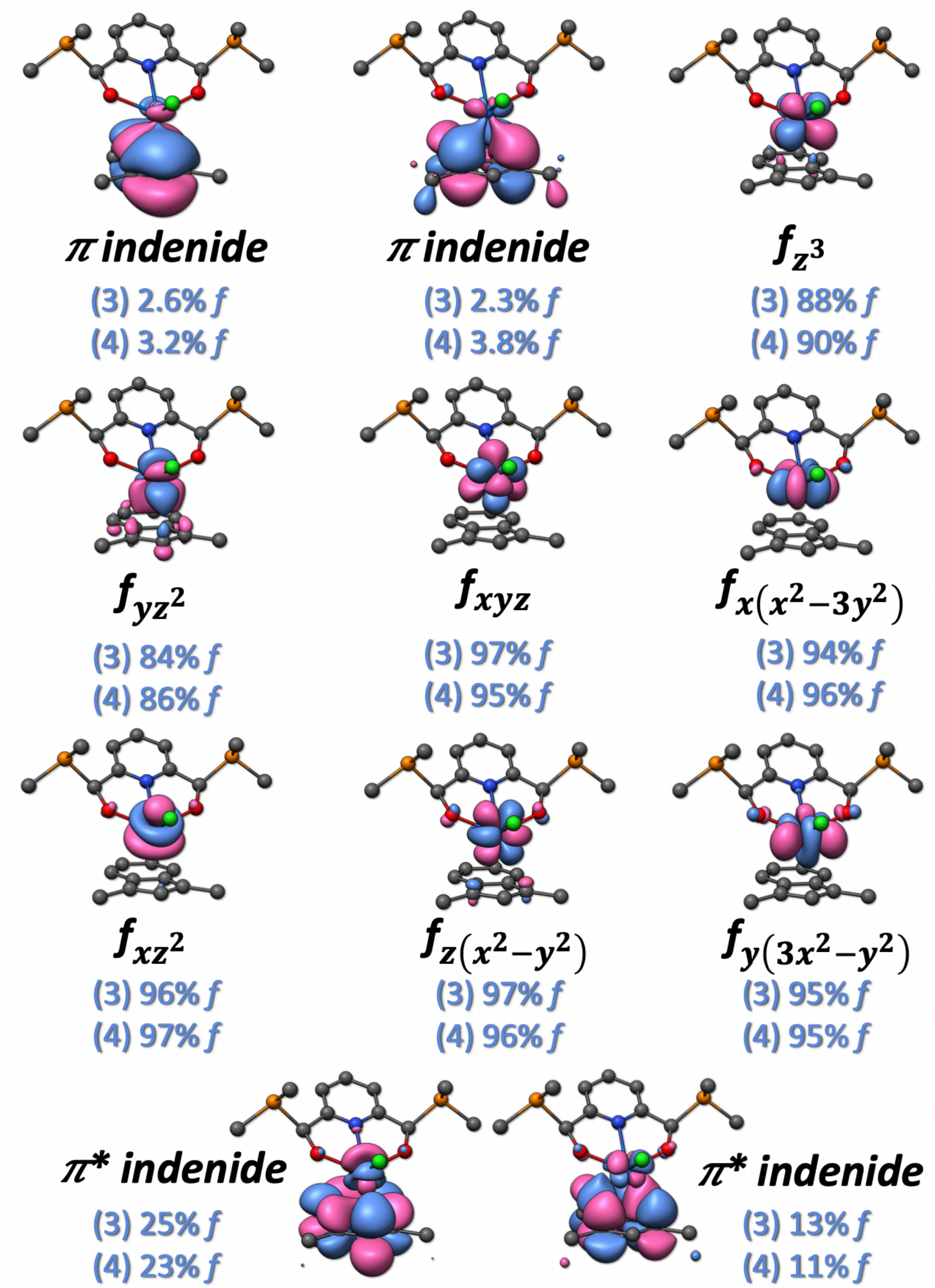

Figure S2. Active orbitals for **3** and **4**. The active space consisted of n + 2 electrons in 11 orbitals (n = 2,3 for U, Np). Isovalue = 0.03.

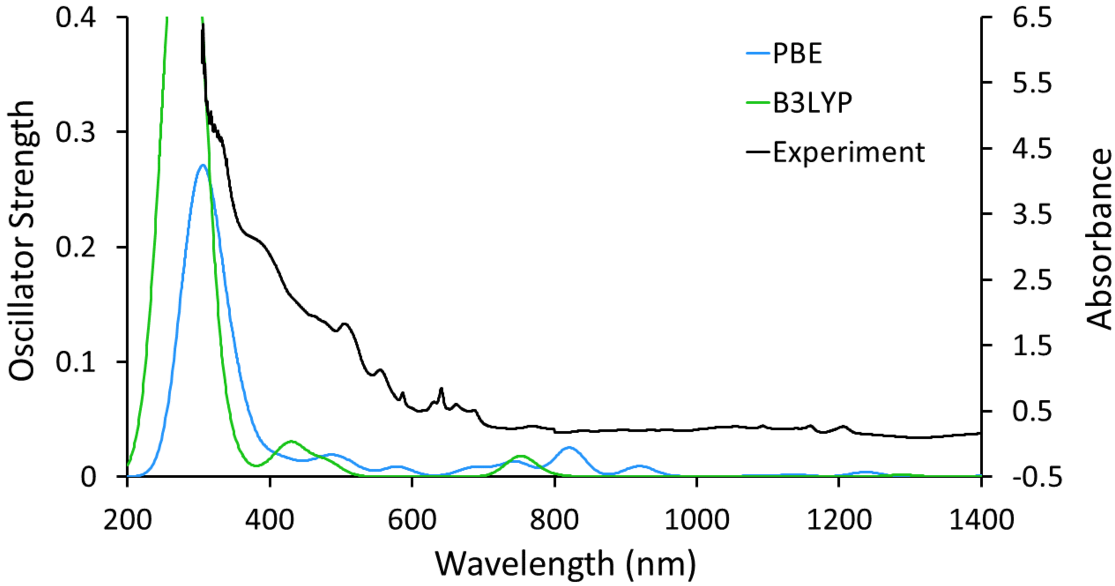

Figure S3. Comparison between experimental and theoretical UV/Vis/NIR spectra for **1.** The theoretical spectra were calculated using the TD-DFT aproximation with the PBE and B3LYP functionals.

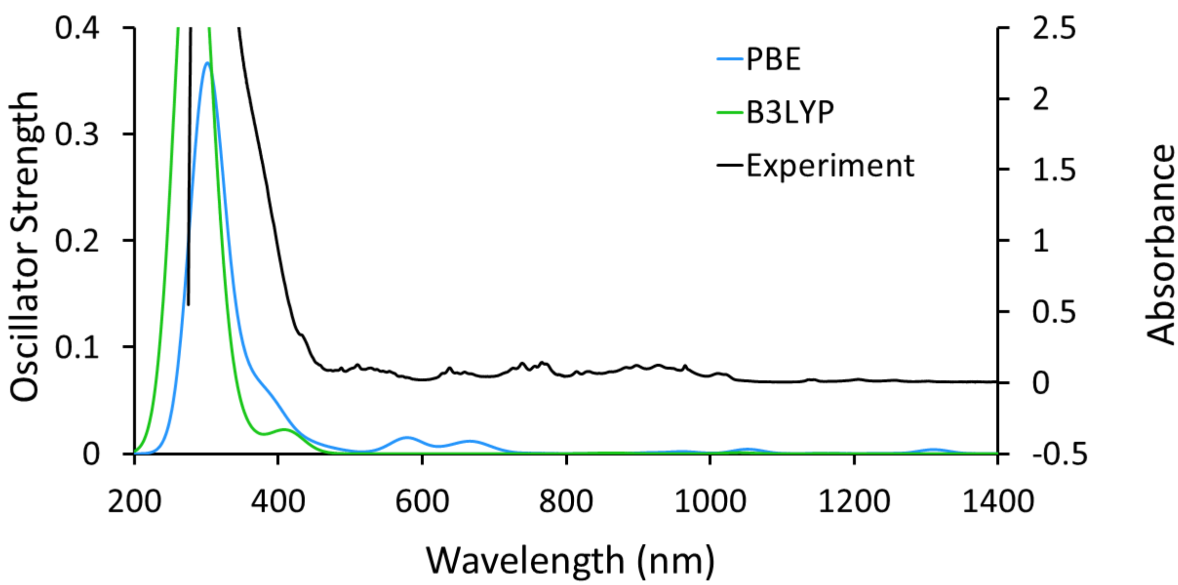

Figure S4. Comparison between experimental and theoretical UV/Vis/NIR spectra for **2.** The theoretical spectra were calculated using the TD-DFT aproximation with the PBE and B3LYP functionals.

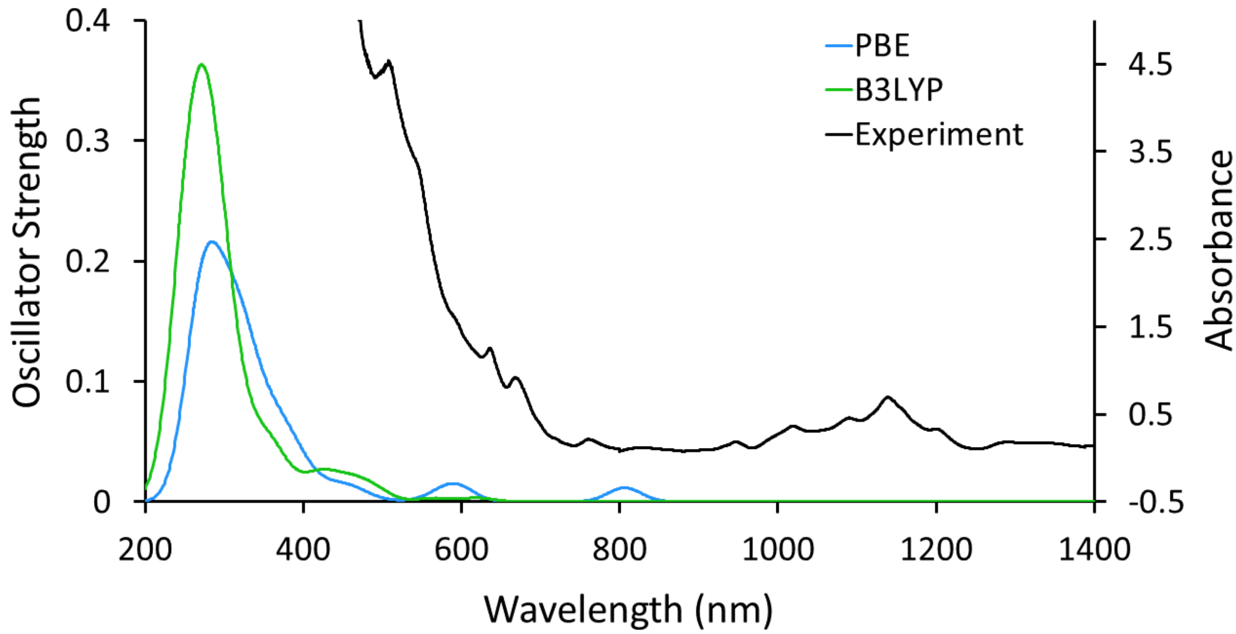

Figure S5. Comparison between experimental and theoretical UV/Vis/NIR spectra for **3**. The theoretical spectra were calculated using the TD-DFT aproximation with the PBE and B3LYP functionals.

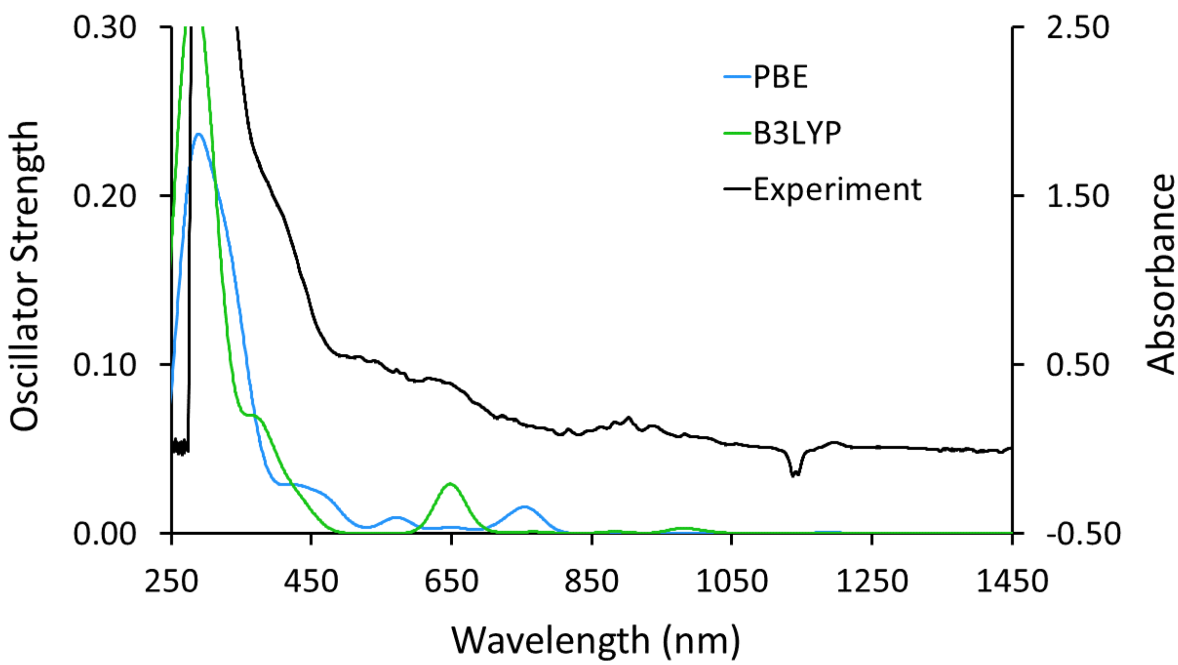

Figure S6. Comparison between experimental and theoretical UV/Vis/NIR spectra for **4**. The theoretical spectra were calculated using the TD-DFT aproximation with the PBE and B3LYP functionals.

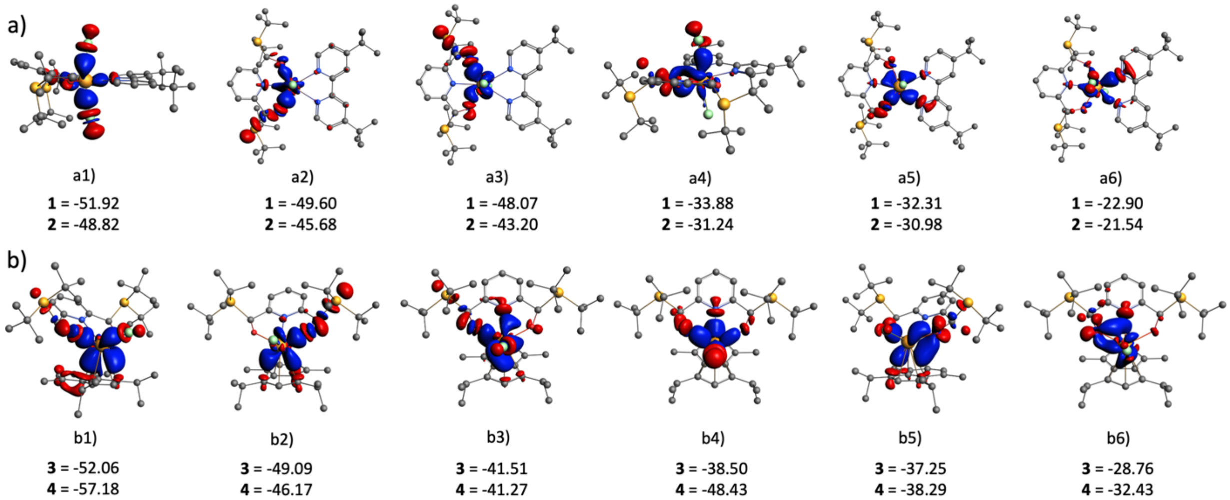

Figure S7. Deformation density plots from the ETS-NOCV analsys for a) dtbpy containing systems and b) indenide complexes. All the values are in kcal/mol.

3. Supplementary Data

3.1 NMR Data

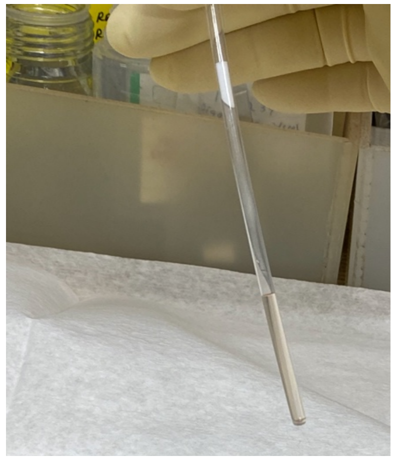

Figure S8. Picture of the NMR sample of ($^{(tBu2P)}$ONO)$NpCl_2$(dtbpy), **2**, taken in C_6D_6.

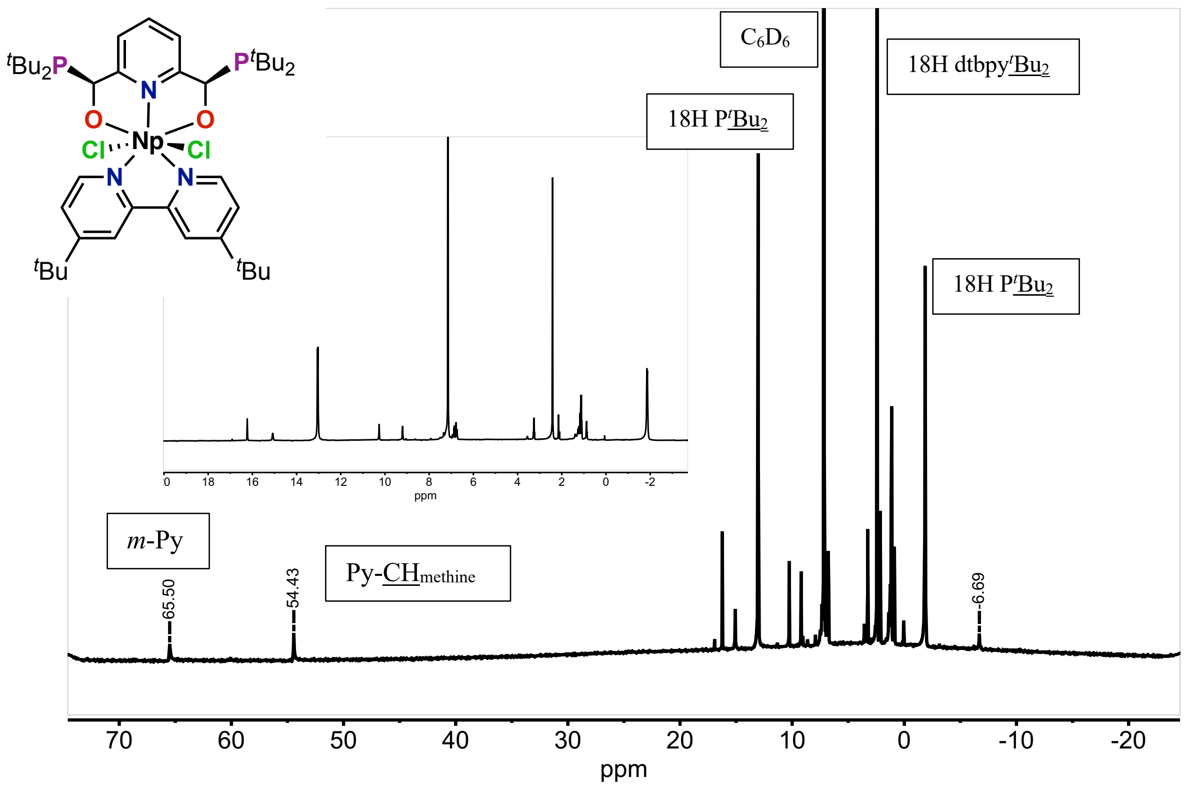

Figure S9. ^{1}H NMR spectrum of ($^{(tBu2P)}$ONO)$NpCl_2$(dtbpy), **2**, obtained in C_6D_6 (4.1 mM).

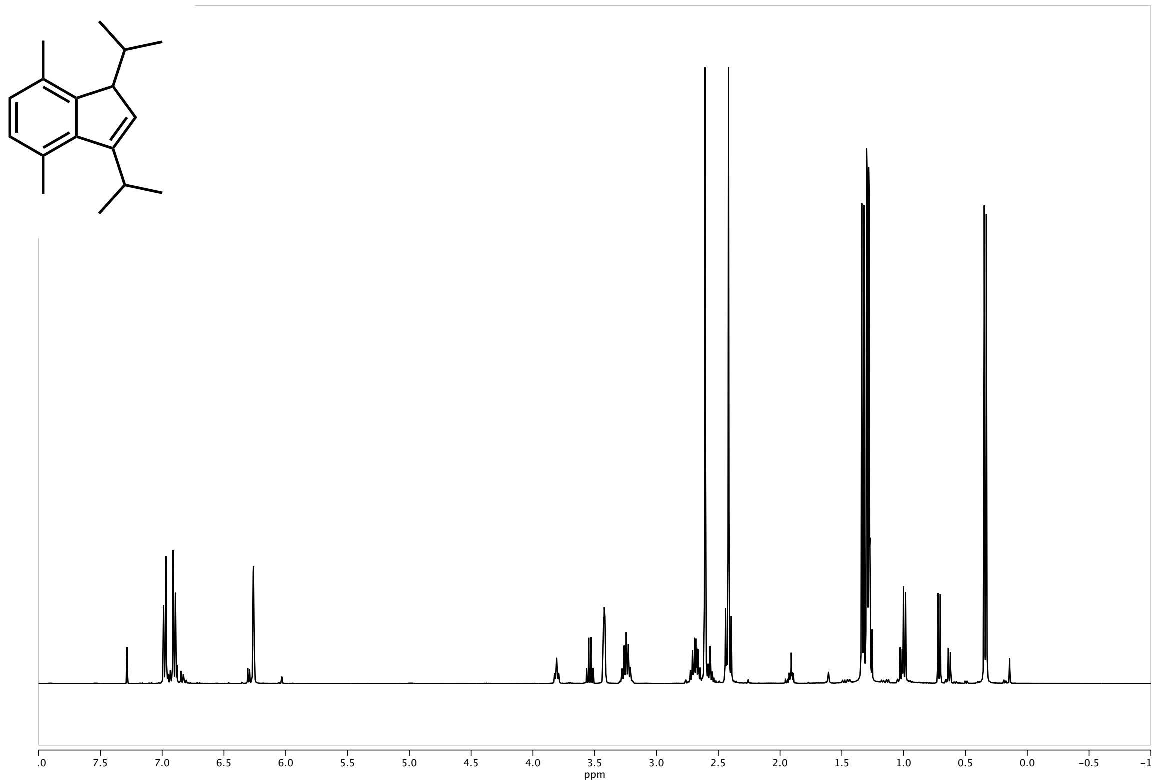

Figure S10. [1]H NMR spectrum of 4,7-dimethyl-1,3-bis(1-methylethyl)-1*H*-indene obtained in C*D*Cl$_3$. Note the multiple isomeric configurations observable by [1]H NMR.

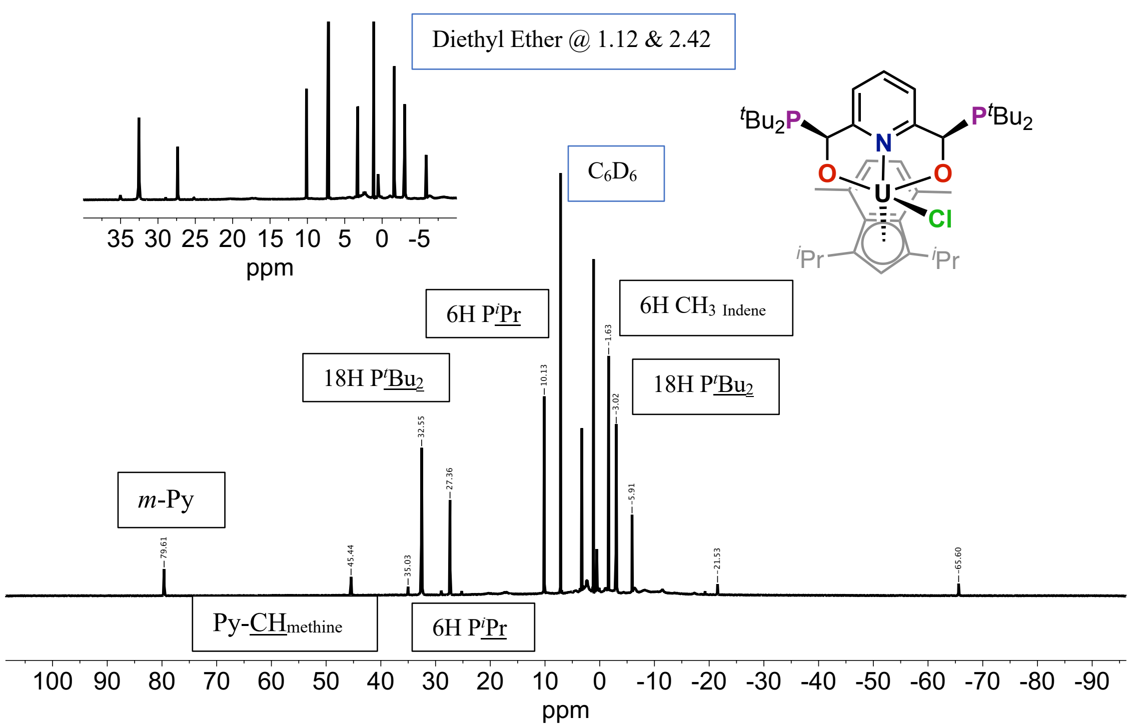

Figure S11. [1]H NMR spectrum of (1,3-iPr$_2$-4,7-Me$_2$-C$_9$H$_3$)($^{(tBu2P)}$ONO)UCl, **3**, obtained in C_6D_6.

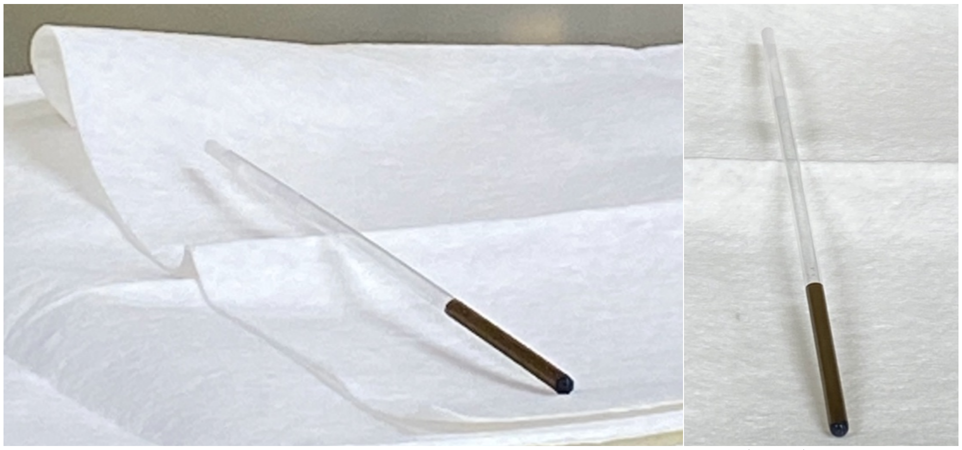

Figure S12. Pictures of the NMR sample of (1,3-iPr$_2$-4,7-Me$_2$-C$_9$H$_3$)($^{(tBu2P)}$ONO)NpCl, **4**, taken in C$_6$D$_6$.

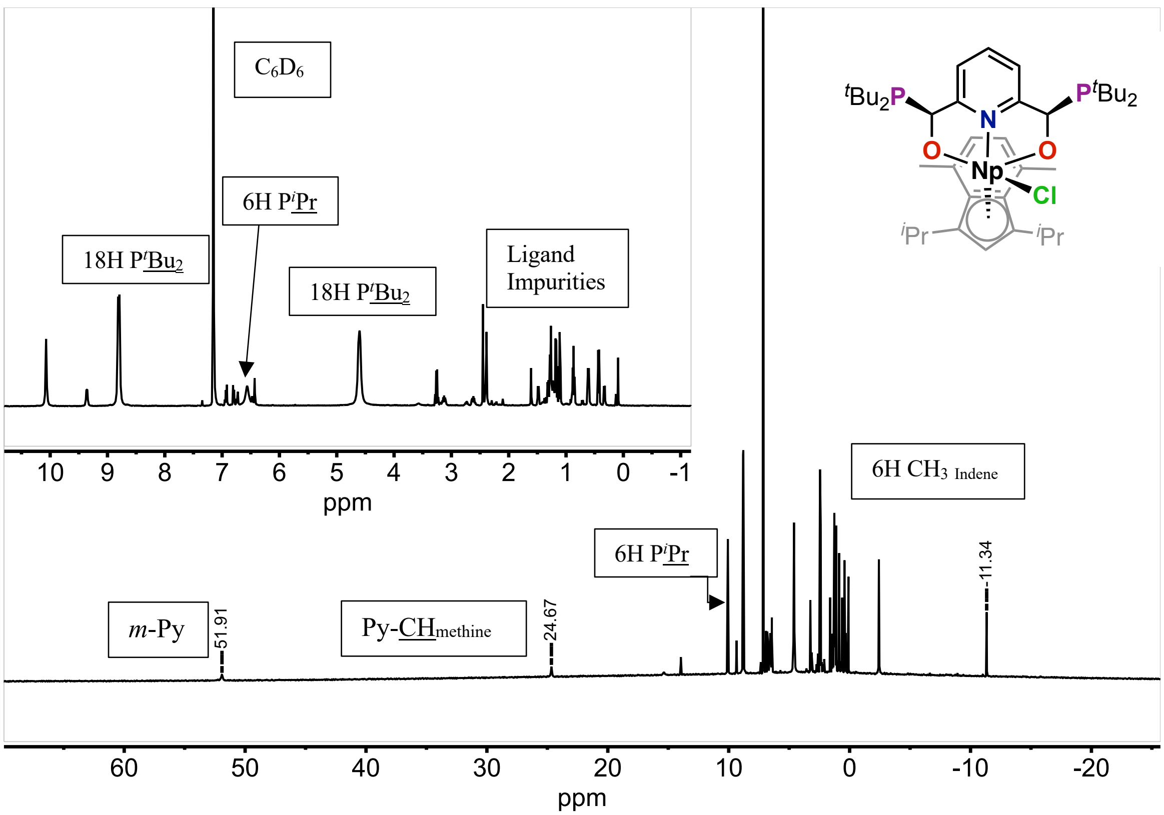

Figure S13. [1]H NMR spectrum of(1,3-iPr$_2$-4,7-Me$_2$-C$_9$H$_3$)($^{(tBu2P)}$ONO)NpCl, **4**, obtained in C$_6$D$_6$ (5.5 mM).

Table S24. Comparison of ^{31}P NMR resonances.

Complex	NMR Shift (δ, ppm)	Ref.
($^{(tBu2P)}$ONO)UCl$_2$(dtbpy), **1**	86.0	4
($^{(tBu2P)}$ONO)NpCl$_2$(dtbpy), **2**	79.3	This work
(1,3-iPr$_2$-4,7-Me$_2$-C$_9$H$_3$)($^{(tBu2P)}$ONO)UCl, **3**	81.8	This work
(1,3-iPr$_2$-4,7-Me$_2$-C$_9$H$_3$)($^{(tBu2P)}$ONO)NpCl, **4**	72.7	This work

3.2 UV/Vis/NIR Data

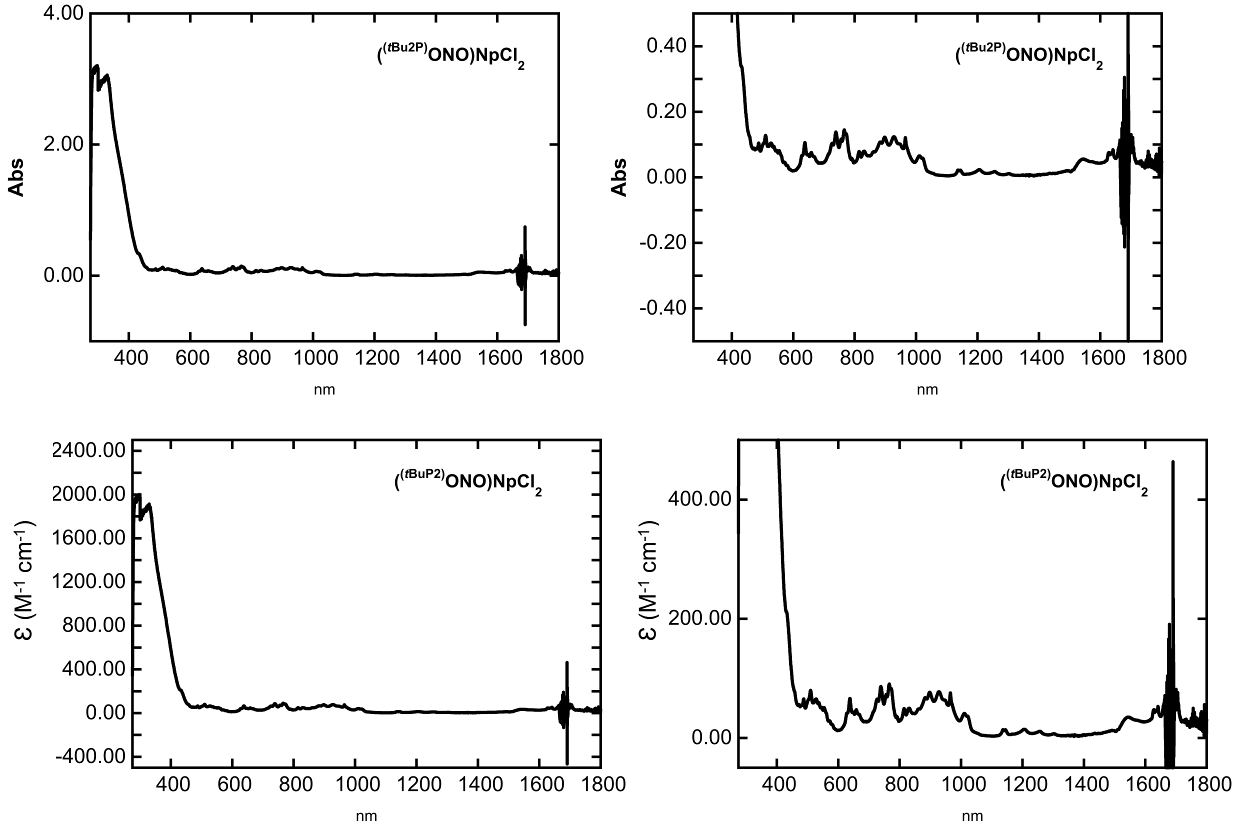

Figure S14. UV/Vis/NIR spectrum of ($^{(tBu2P)}$ONO)NpCl$_2$(dtbpy), **2**, taken in C_6H_6:C_6D_6 60:40 (1.6 mM) in absorbance (top) and molar absorptivity (bottom).

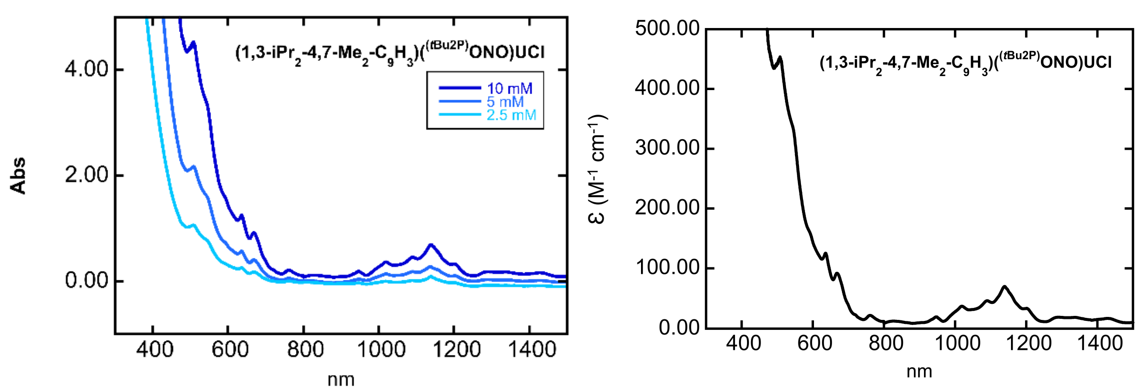

Figure S15. UV/Vis/NIR spectrum of (1,3-iPr$_2$-4,7-Me$_2$-C_9H_3)($^{(tBu2P)}$ONO)UCl, **3**, in toluene at varying concentrations in absorbance (left) and molar absorptivity (right).

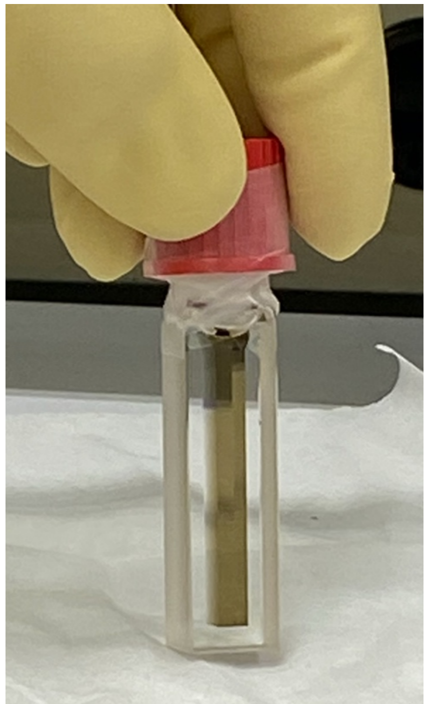

Figure S16. Picture of the UV/Vis/NIR sample of (1,3-iPr$_2$-4,7-Me$_2$-C$_9$H$_3$)($^{(tBu2P)}$ONO)NpCl, **4**, taken in C_6H_6:C_6D_6 60:40 (1.2 mM).

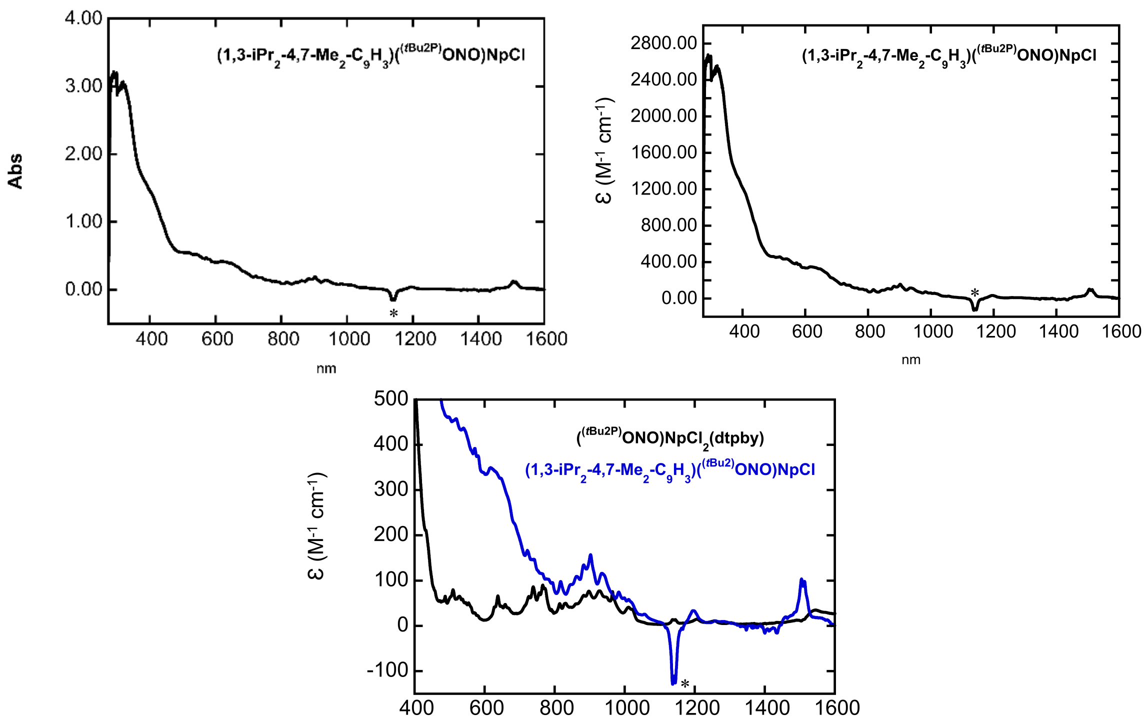

Figure S17. UV/Vis/NIR Spectrum of (1,3-iPr$_2$-4,7-Me$_2$-C$_9$H$_3$)($^{(tBu2P)}$ONO)NpCl, **4**, taken in C_6H_6:C_6D_6 60:40 (1.2 mM) in absorbance (top left) and molar absorptivity (top right). Bottom is a comparison between complexes **2** and **4**. *Indicates a known artefact of the instrument.

3.3 Pictures of Reactions and Crystalline Material of 1 and 4

Figure S18. The mixture of $(dme)_2NpCl_4$ and 2,6-pyridine dicarboxaldehyde in THF results in a pale pink solution.

Figure S19. The addition of $^{t}Bu_2PSiMe_3$ (2 equiv) to the pink solution shown in **Figure S18** results in an immediately color change to bright yellow.

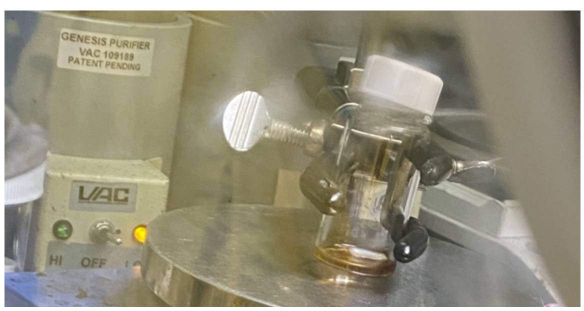

Figure S20. The resulting yellow powder from **Figure S19** was resuspended in fluorobenzene. The addition of dtbpy to this mixture results in a color change to peach, and from this solution crystalline material was collected (**Figure S21**).

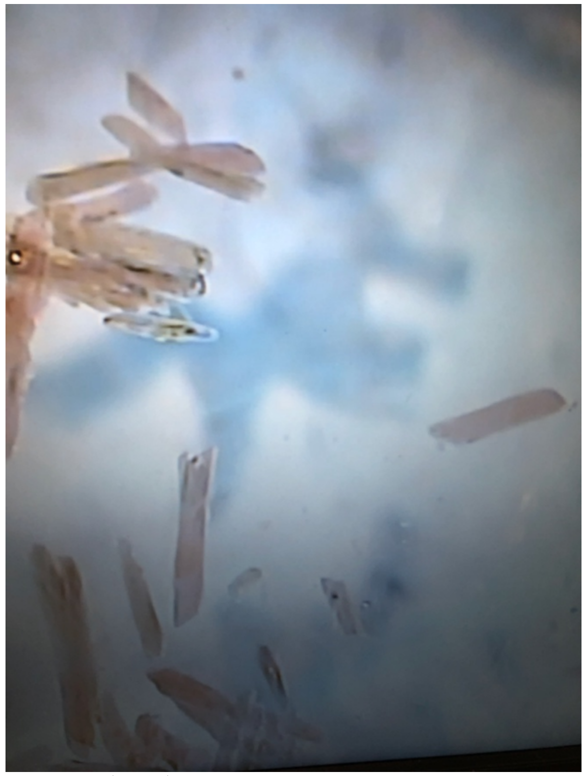

Figure S21. Pale peach crystals of $(^{(t\mathrm{Bu2P})}\mathrm{ONO})\mathrm{NpCl_2(dtbpy)}$, **2**.

Figure S22. The initial steps in the synthesis of $(1,3\text{-}i\mathrm{Pr_2}\text{-}4,7\text{-}\mathrm{Me_2}\text{-}\mathrm{C_9H_3})(^{(t\mathrm{Bu2P})}\mathrm{ONO})\mathrm{NpCl}$, **4**, are reminiscent of the reactions observed in **Figures S18, S19**. The addition of in-situ deprotonated $1,3\text{-}i\mathrm{Pr_2}\text{-}4,7\text{-}\mathrm{Me_2}\text{-}\mathrm{C_9H_3}$ **(**using (trimethylsilyl)methyl sodium ($\mathrm{Na\text{-}CH_2Si(Me)_3}$) to this yellow solution results in the formation of a dark solution.

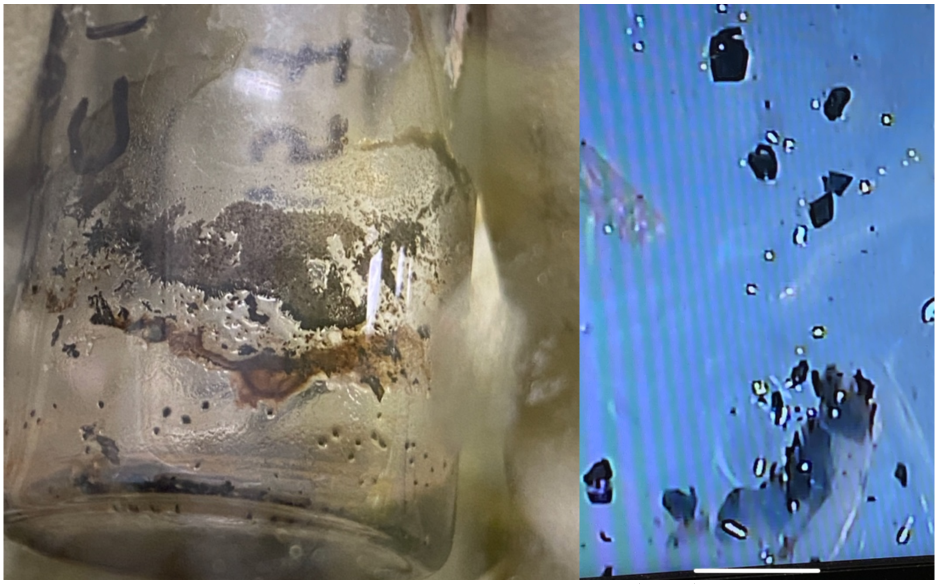

Figure S23. Dark crystalline material (1,3-iPr$_2$-4,7-Me$_2$-C$_9$H$_3$)($^{(tBu2P)}$ONO)NpCl, **4**, observed in a vial (left) and under a microscope (right).

4. Isolation of an Intermediate Product

Care must be taken to allow sufficient time for TMS-Cl generation and An-O bond formation to occur. An intermediate complex arising from incomplete formation of ($^{(tBu2P)}$ONO) forms, giving products from the loss of a single TMS-Cl. This intermediate was identified by SC-XRD as ($^{(OTMS)}$PNO^{tBu})UCl_2(η^5-C_9H_3-1,3-(iPr$_2$)-4,7-Me$_2$ (**3b**, **Figure S24**, $^{(OTMS)}$PNO^{tBu} = 2-((trimethylsiloxy)(*tert*-butylphosphino)-methyl-6-((*tert*-butylphosphino-methanolato)pyridine)). Complex **3b** is reminiscent of the previously reported ($^{(OTMS)}$PNO^{tBu})UCl_3(dtbpy),[4] and is a rational intermediate in the formation of **3**. Efforts to isolate the pure complex of **3b** were unsuccessful as the isolation of this complex under normal reaction conditions was inconsistent. Further experiments to independently isolate **3b** led to the isolation of **3** instead. Due to this conditions, further characterization of **3b** beyond SC-XRD was not possible. The change in supporting ligand (indenide vs dtbpy) does not drastically alter the bond lengths and angles between **3b** and ($^{(OTMS)}$PNO^{tBu})UCl_3(dtbpy) (**Table S25**), suggesting the change in supporting ligand does not significantly affect the electronic structure of these complexes. However, the intermediate, **3b**, has contracted U-O bonds distances and elongated U-N_{pyr} and U-centroid bond distances when compared to **3**. As **3b** cannot be isolated consistently, focus was then shifted to adapting this chemistry to neptunium.

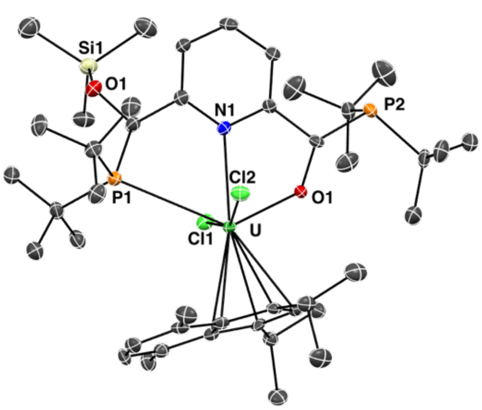

Figure S24. Solid-state structure of **3b**, a likely intermediate in the formation of **3**, presented at 50% probability ellipsoids.

Table S25. Select shared bond distances (Å) and angles (°) for ($^{(OTMS)}$PNO^{tBu})UCl$_2$(η^5-C$_9$H$_3$-1,3-(iPr$_2$)-4,7-Me$_2$ in comparison to ($^{(OTMS)}$PNO^{tBu})U-Cl$_3$(dtbpy).[4]

Å , ∠ (˚)	**($^{(OTMS)}$PNO^{tBu})U-Cl$_3$(dtbpy)[4]**	**($^{(OTMS)}$PNO^{tBu})UCl$_2$(η^5-C$_9$H$_3$-1,3-(iPr$_2$)-4,7-Me$_2$ (3b)**
U-O1	2.069(5)	2.081(3)
U-P1	3.220(3)	3.257(2)
U-Cl1	2.658(3)	2.646(2)
U-Cl2	2.663(3)	2.629(2)
U-N$_{pyr}$	2.648(6)	2.571(3)
U-Centroid	N/A	2.501
Cl1-U-Cl2	144.21(6)	157.08(3)
O1-U-P1	127.46(14)	131.10(8)
N$_{pyr}$-U-O1	64.82(18)	66.25(11)
N$_{pyr}$-U-P1	62.92(13)	64.87(8)

5. Single Crystal X-ray Diffraction Data

5.1 CCDC Deposition, 2297381-2297385.

($^{(tBu2P)}$ONO)UCl_2(dtbpy), **1**, (*P*-1 unit cell): *2297381*

($^{(tBu2P)}$ONO)$NpCl_2$(dtbpy), **2**: *2297382*

(1,3-iPr_2-4,7-Me_2-C_9H_3)($^{(tBu2P)}$ONO)UCl, **3**: *2297383*

($^{(OTMS)}$PNO^{tBu})UCl_2(η^5-C_9H_3-1,3-($CHMe_2$)$_2$-4,7-Me_2, **3b**: *2297384*

(1,3-iPr_2-4,7-Me_2-C_9H_3)($^{(tBu2P)}$ONO)NpCl, **4**: *2297385*

5.2 Crystallography Tables: Refinement Details, Bond Distances (Å), and Angles (°)

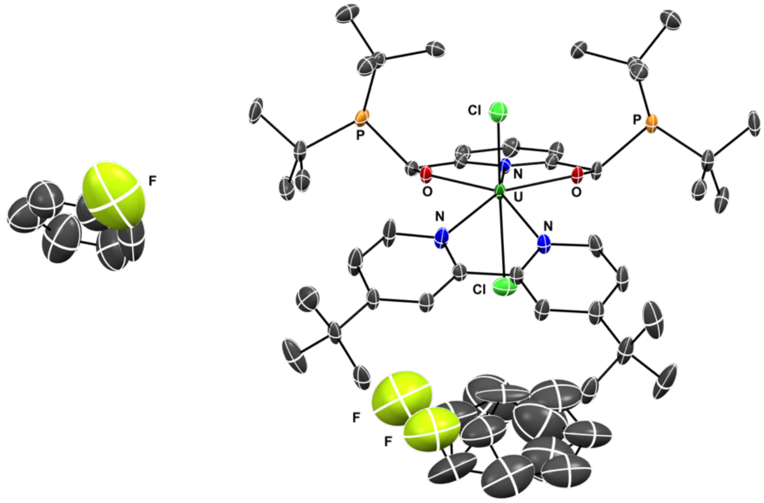

Figure S25. Crystal structure of ($^{(tBu2P)}$ONO)UCl_2(dtbpy), **1**, (P-1 unit cell).

Table S26. Crystal data and structure refinement for ($^{(tBu2P)}$ONO)UCl_2(dtbpy), **1**.

Identification code	**mesoONOUBPYCl2**
Empirical formula	$C_{53}H_{75}Cl_2F_2N_3O_2P_2U$
Formula weight	1195.03
Temperature/K	101.00
Crystal system	triclinic
Space group	P-1
a/Å	14.7477(5)
b/Å	14.9676(5)
c/Å	15.9026(5)
α/°	76.1970(10)
β/°	69.6960(10)
γ/°	73.7070(10)
Volume/Å^3	3120.84(18)
Z	2
ρ_{calc}g/cm^3	1.272
μ/mm^{-1}	2.779
F(000)	1208.0
Crystal size/mm^3	0.22 × 0.17 × 0.14
Radiation	MoKα (λ = 0.71073)
2Θ range for data collection/°	4.286 to 52.044
Index ranges	-18 ≤ h ≤ 18, -18 ≤ k ≤ 18, -19 ≤ l ≤ 19
Reflections collected	43106
Independent reflections	12283 [R_{int} = 0.0353, R_{sigma} = 0.0345]
Data/restraints/parameters	12283/240/619
Goodness-of-fit on F^2	1.106
Final R indexes [I>=2σ (I)]	R_1 = 0.0356, wR_2 = 0.0848
Final R indexes [all data]	R_1 = 0.0395, wR_2 = 0.0861
Largest diff. peak/hole / e Å^{-3}	2.00/-0.95

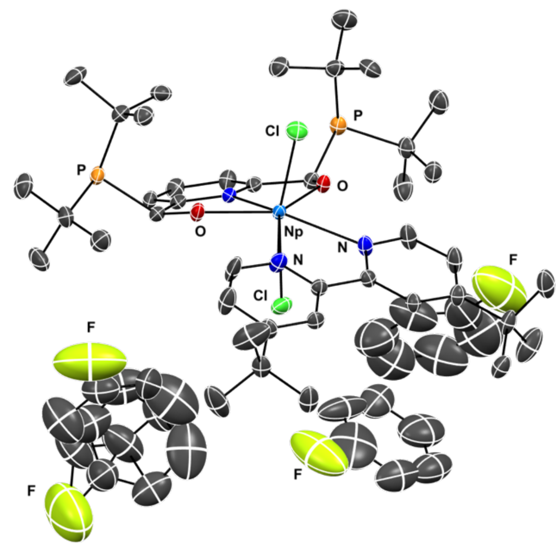

Figure S26. Crystal structure of ($^{(tBu2P)}$ONO)NpCl_2(dtbpy), **2**.

Table S27. Crystal data and structure refinement for ($^{(tBu2P)}$ONO)NpCl_2(dtbpy), **2**.

Identification code	**NpTempint2**
Empirical formula	$C_{59}H_{80}Cl_2F_2N_3NpO_2P_2$
Formula weight	1271.10
Temperature/K	100.0
Crystal system	triclinic
Space group	P-1
a/Å	14.7455(19)
b/Å	15.1440(18)
c/Å	15.9601(18)
α/°	76.118(6)
β/°	69.493(6)
γ/°	72.912(6)
Volume/Å^3	3153.2(7)
Z	2
ρ_{calc}g/cm^3	1.339
μ/mm^{-1}	1.829
F(000)	1292.0
Crystal size/mm^3	0.31 × 0.2 × 0.09
Radiation	MoKα (λ = 0.71073)
2Θ range for data collection/°	4.256 to 53.464
Index ranges	-15 ≤ h ≤ 18, -17 ≤ k ≤ 19, -19 ≤ l ≤ 20
Reflections collected	35734
Independent reflections	13247 [R_{int} = 0.0414, R_{sigma} = 0.0475]
Data/restraints/parameters	13247/156/674
Goodness-of-fit on F^2	1.100
Final R indexes [I>=2σ (I)]	R_1 = 0.0420, wR_2 = 0.1075
Final R indexes [all data]	R_1 = 0.0481, wR_2 = 0.1097
Largest diff. peak/hole / e Å^{-3}	1.85/-1.48

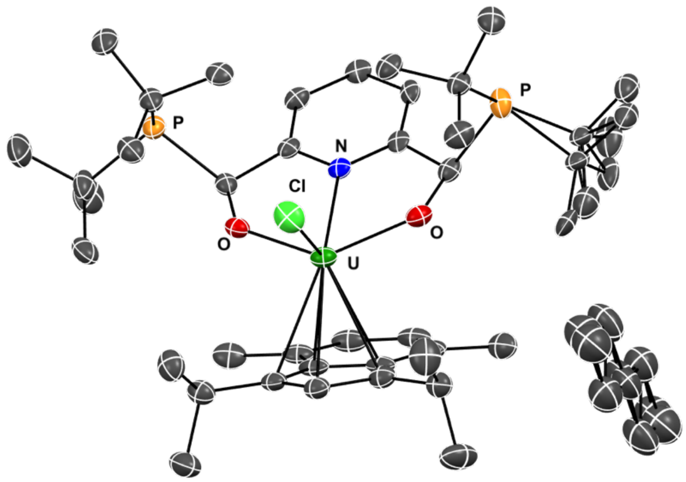

Figure S27. Crystal structure of (1,3-iPr$_2$-4,7-Me$_2$-C$_9$H$_3$)($^{(tBu2P)}$ONO)UCl, **3**.

Table S28. Crystal data and structure refinement for (1,3-iPr$_2$-4,7-Me$_2$-C$_9$H$_3$)($^{(tBu2P)}$ONO)UCl, **3**.

Identification code	**mesoONOUIndCl**
Empirical formula	$C_{85}H_{140}Cl_2N_2O_4P_4U_2$
Formula weight	1924.82
Temperature/K	100.00
Crystal system	monoclinic
Space group	$P2_1/n$
a/Å	14.5847(9)
b/Å	15.9526(9)
c/Å	20.0810(12)
α/°	90
β/°	107.634(4)
γ/°	90
Volume/Å^3	4452.6(5)
Z	2
ρ_{calc}g/cm^3	1.436
μ/mm^{-1}	3.810
F(000)	1948.0
Crystal size/mm^3	0.15 × 0.15 × 0.1
Radiation	MoKα (λ = 0.71073)
2Θ range for data collection/°	3.982 to 55.4
Index ranges	$-15 \le h \le 18, -20 \le k \le 20, -26 \le l \le 26$
Reflections collected	48044
Independent reflections	10273 [R_{int} = 0.0847, R_{sigma} = 0.0640]
Data/restraints/parameters	10273/9/515
Goodness-of-fit on F^2	1.016
Final R indexes [I>=2σ (I)]	R_1 = 0.0362, wR_2 = 0.0781
Final R indexes [all data]	R_1 = 0.0681, wR_2 = 0.0877
Largest diff. peak/hole / e Å^{-3}	2.52/-1.03

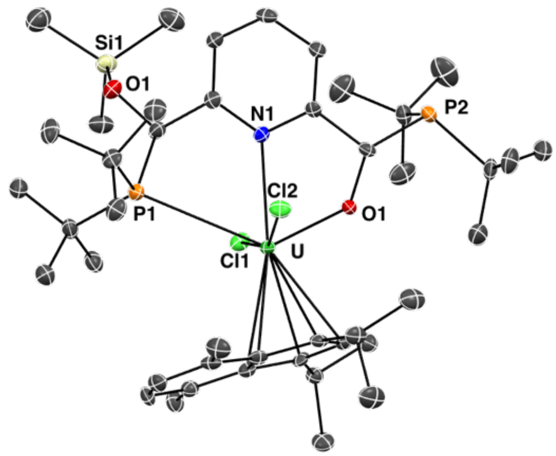

Figure S28. Crystal structure of ($^{(OTMS)}$PNO^{tBu})UCl$_2$(η^5-C$_9$H$_3$-1,3-(CHMe$_2$)$_2$-4,7-Me$_2$), **3b**.

Table S29. Crystal data and structure refinement for ($^{(OTMS)}$PNO^{tBu})UCl$_2$(η^5-C$_9$H$_3$-1,3-(CHMe$_2$)$_2$-4,7-Me$_2$), **3b**.

Identification code	**IndTempIntermediate_a**
Empirical formula	$C_{48}H_{85}Cl_2NO_2P_2SiU$
Formula weight	1107.12
Temperature/K	100.0
Crystal system	monoclinic
Space group	$P2_1/n$
a/Å	13.7880(7)
b/Å	18.7203(10)
c/Å	20.9908(11)
α/°	90
β/°	103.403(3)
γ/°	90
Volume/Å^3	5270.5(5)
Z	4
ρ_{calc}g/cm^3	1.395
μ/mm^{-1}	3.300
F(000)	2264.0
Crystal size/mm^3	0.35 × 0.15 × 0.12
Radiation	MoKα (λ = 0.71073)
2Θ range for data collection/°	4.002 to 53.462
Index ranges	$-17 \le h \le 17$, $-20 \le k \le 23$, $-26 \le l \le 26$
Reflections collected	59036
Independent reflections	11192 [R_{int} = 0.0984, R_{sigma} = 0.0755]
Data/restraints/parameters	11192/0/537
Goodness-of-fit on F^2	1.041
Final R indexes [I>=2σ (I)]	R_1 = 0.0360, wR_2 = 0.0733
Final R indexes [all data]	R_1 = 0.0607, wR_2 = 0.0798
Largest diff. peak/hole / e Å^{-3}	1.19/-0.73

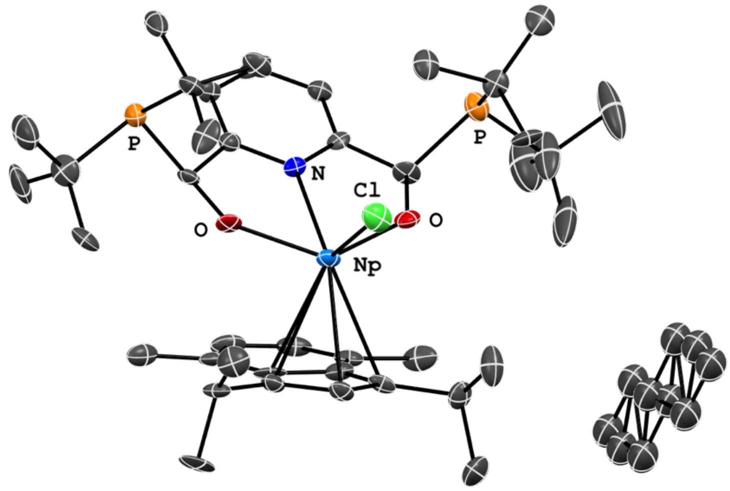

Figure S29. Crystal structure of (1,3-iPr$_2$-4,7-Me$_2$-C$_9$H$_3$)($^{(t\text{Bu2P})}$ONO)NpCl, **4**.

Table S30. Crystal data and structure refinement for (1,3-iPr$_2$-4,7-Me$_2$-C$_9$H$_3$)($^{(t\text{Bu2P})}$ONO)NpCl, **4**.

Identification code	**mesoONONpInd_5**
Empirical formula	$C_{42.5}H_{70}ClNNpO_2P_2$
Formula weight	961.38
Temperature/K	100.00
Crystal system	monoclinic
Space group	$P2_1/n$
a/Å	14.5847(9)
b/Å	15.9526(9)
c/Å	20.0810(12)
α/°	90
β/°	107.634(4)
γ/°	90
Volume/Å^3	4452.6(5)
Z	4
ρ_{calc}g/cm^3	1.434
μ/mm^{-1}	2.499
F(000)	1952.0
Crystal size/mm^3	0.15 × 0.15 × 0.1
Radiation	MoKα (λ = 0.71073)
2Θ range for data collection/°	4.84 to 52.042
Index ranges	$-18 \le h \le 17$, $0 \le k \le 19$, $0 \le l \le 24$
Reflections collected	8432
Independent reflections	8432 [R_{int} = ?, R_{sigma} = 0.0619]
Data/restraints/parameters	8432/87/464
Goodness-of-fit on F^2	1.176
Final R indexes [I>=2σ (I)]	R_1 = 0.0604, wR_2 = 0.1144
Final R indexes [all data]	R_1 = 0.0919, wR_2 = 0.1325
Largest diff. peak/hole / e Å^{-3}	1.88/-1.70

6. References

1. J. L. Kiplinger, D. E. Morris, B. L. Scott and C. J. Burns, *Organometallics*, 2002, **21**, 5978-5982.
2. S. D. Reilly, J. L. Brown, B. L. Scott and A. J. Gaunt, *Dalton Trans.*, 2014, **43**, 1498-1501.
3. G. P. McGovern, F. Hung-Low, J. W. Tye and C. A. Bradley, *Organometallics*, 2012, **31**, 3865-3879.
4. S. H. Carpenter, B. S. Billow and A. M. Tondreau, *Organometallics*, 2021, **40**, 2389-2393.
5. J. E. Radcliffe, A. S. Batsanov, D. M. Smith, J. A. Scott, P. W. Dyer and M. J. Hanton, *ACS Catal.*, 2015, **5**, 7095-7098.
6. C. A. P. Goodwin, M. T. Janicke, B. L. Scott and A. J. Gaunt, *J. Am. Chem. Soc.*, 2021, **143**, 20680-20696.
7. Service, B. I. *Version 2010.1.0.0*, Bruker AXS Inc.: Madison, WI, 2010.
8. *SAINT Plus, Data Reduction Software. Version 7.68A*, Bruker AXS Inc.: Madison, WI, 2009.
9. G. M. Sheldrick, *Acta Crystallogr., Sect. A: Found. Crystallogr.*, 2008, **64**, 112-122.
10. Sheldrick, G. M. *SADABS*, University of Göttingen: Germany, 2005.
11. G. M. Sheldrick, *Acta Crystallogr., Sect. C: Struct. Chem.*, 2015, **71**, 3-8.
12. *APEX2, Data Refinement Software. Version 2010.1-2*, Bruker AXS Inc.: Madison, Wi, 2010.
13. Olex2 1.2 (compiled 2014.06.27 svn.r2953 for OlexSys, GUI svn.r4855).
14. O. V. Dolomanov, L. J. Bourhis, R. J. Gildea, J. A. K. Howard and H. Puschmann, *J. Appl. Crystallogr.*, 2009, **42**, 339-341.
15. R. F. Rüger, M.; Trnka, T.; Yakovlev, A.; van Lenthe, E.; Philipsen, P.; van Vuren, T.; Klumpers, B.; Soini, T., *AMS, SCM,Theoretical Chemistry; Vrije Universiteit: Amsterdam, The Netherlands, 2021*.
16. J. P. Perdew, K. Burke and M. Ernzerhof, *Phys. Rev. Lett.*, 1996, **77**, 3865-3868.
17. A. D. Becke, *J. Chem. Phys.*, 1993, **98**, 5648.
18. C. Lee, W. Yang and R. G. Parr, *Phys. Rev. B: Condens. Matter*, 1988, **37**, 785.
19. E. van Lenthe, J. G. Snijders and E. J. Baerends, *J. Chem. Phys.*, 1996, **105**, 6505-6516.
20. E. D. B. Glendening, J. K.; Reed, A. E.; Carpenter, J. E.; Bohmann, J. A.; Morales, C. M.; Karafiloglou, P.; Landis, C. R.; Weinhold, F. , *Journal*, 2018.
21. M. P. Mitoraj, A. Michalak and T. Ziegler, *J. Chem. Theory Comput.*, 2009, **5**, 962-975.
22. F. Neese, *WIREs Computational Molecular Science*, 2022, **12**, e1606.
23. F. Weigend and R. Ahlrichs, *Phys. Chem. Chem. Phys.*, 2005, **7**, 3297-3305.
24. D. A. Pantazis and F. Neese, *J. Chem. Theory Comput.*, 2011, **7**, 677-684.
25. B. A. Hess, *Phys. Rev. A: Gen. Phys.*, 1986, **33**, 3742.
26. B. O. Roos, P. R. Taylor and E. M. Siegbahn, *Chem. Phys.*, 1980, **48**, 157.
27. C. Angeli, R. Cimiraglia and J.-P. Malrieu, *J. Chem. Phys.*, 2002, **117**, 9138-9153.